(1)

CASTING OF HALIDE AND FLUORIDE ALLOYS FOR LASER WINDOWS

R. T. Newberg
D. W. Readey
H. A. Newborn

Raytheon Research Division
Waltham, Massachusetts 02154

Contract No. F19628-74-C-0148

Quarterly Technical Report No. 1

Period covered 15 March through 14 June 1974

July 15, 1974

Contract Monitor and Alternate
John J. Larkin and Alton Armington
Solid State Sciences Laboratory

Sponsored By

Defense Advanced Research Projects Agency
ARPA Order No. 2669
Monitored by
Air Force Cambridge Research Laboratories

ARPA Order No.
2669

Contract No.
F19628-74-C-0148

Program Code No.
4 D 10

Prin. Investigator and Phone No.
Dr. Dennis Readey (617) 899-8400
ext. 2475

Name of Contractor
Raytheon Research Division

AFCRL Project Scientist and
Alternate and Phone No.
Dr. John J. Larkin and Dr. Alton
Armington (617) 861-4807

Effective Date of Contract
March 15, 1974

Contract Expiration Date
September 14, 1975

Unclassified

SECURITY CLASSIFICATION OF THIS PAGE (When Data Entered)

REPORT DOCUMENTATION PAGE	READ INSTRUCTIONS BEFORE COMPLETING FORM
1. REPORT NUMBER	2. GOVT ACCESSION NO. AD-A015 858	3. RECIPIENT'S CATALOG NUMBER
4. TITLE (and Subtitle) CASTING OF HALIDE AND FLUORIDE ALLOYS FOR LASER WINDOWS	5. TYPE OF REPORT & PERIOD COVERED Quarterly Technical 3/15/74-6/14/74
	6. PERFORMING ORG. REPORT NUMBER S-1714
7. AUTHOR(s) R.T. Newberg, D.W. Readey, H.A. Newborn	8. CONTRACT OR GRANT NUMBER(s) F19628-74-C-0148
9. PERFORMING ORGANIZATION NAME AND ADDRESS Raytheon Research Division Waltham, MA 02154	10. PROGRAM ELEMENT, PROJECT, TASK AREA & WORK UNIT NUMBERS Program Code No. 4 D 10
11. CONTROLLING OFFICE NAME AND ADDRESS Advanced Research Projects Agency Arlington, Va. 22209	12. REPORT DATE July 15, 1974
	13. NUMBER OF PAGES 77
14. MONITORING AGENCY NAME & ADDRESS(if different from Controlling Office) Air Force Cambridge Research Labs. L.G. Hanscom Field Bedford, Mass. 01730	15. SECURITY CLASS. (of this report) Unclassified
	15a. DECLASSIFICATION/DOWNGRADING SCHEDULE

16. DISTRIBUTION STATEMENT (of this Report)

APPROVED FOR PUBLIC RELEASE; DISTRIBUTION IS UNLIMITED (A)

17. DISTRIBUTION STATEMENT (of the abstract entered in Block 20, if different from Report)

18. SUPPLEMENTARY NOTES

19. KEY WORDS (Continue on reverse side if necessary and identify by block number)

Infrared Materials
Alkali Halides
Alkaline Earth Fluorides
Casting
Optical Properties

20. ABSTRACT (Continue on reverse side if necessary and identify by block number)

During the first quarter of this program several important goals were accomplished. The problem of residual strain in castings of halides (KCl and $SrCl_2$ doped KCl) and fluorides (pure CaF_2) has been largely overcome by using proper annealing and cooling procedures. Large castings (5 1/2 in. diameter) of CaF_2 have been produced with low optical absorption coefficients at 5.25 μm. Semi-quantitative analysis of absorption coefficients and scattering centers has been initiated with preliminary results showing a correlation between the two. Reactive atmosphere processing (RAC) of castings has begun.

DD FORM 1 JAN 73 1473 EDITION OF 1 NOV 65 IS OBSOLETE

Unclassified

SECURITY CLASSIFICATION OF THIS PAGE (When Data Entered)

TECHNICAL PROGRAM SUMMARY

The primary objectives of this program are to complete the investigation of the properties of fusion cast $SrCl_2$-KCl alloys and to investigate the fabrication and properties of alkaline earth fluoride castings for high power laser window applications.

During this past quarter, time-temperature-transformation curves for precipitation and attendant hardness reduction in KCl-$SrCl_2$ alloys have been completed. The results indicate that for less than about 800 ppm $SrCl_2$ in solid solution, it should be possible to cool alloys from the melting point to room temperature without precipitation.

Attempts were made to determine the thermal conductivity of KCl-$SrCl_2$ alloys and were unsuccessful due to difficulties with sample size and preparation.

A serious problem with casting these materials which have large volume changes upon freezing and large thermal expansion coefficients is the residual stress in the ingots after cooling. During this quarter an annealing and cooling procedure was successfully developed which removes the major part of the residual stress in KCl castings.

Reactive atmosphere processing (RAP) of "reagent" grade KCl starting material was successful in removing impurities which produced strong absorption bands in the IR. However, the broad absorption centered at about 10 μm which produces strong 10.6 μm absorption was not eliminated completely in these early runs.

It was observed that many samples which do not exhibit the broad 10 μm absorption band still may have a high 10.6 μm absorption coefficient. Preliminary data indicate that this high apparent absorption coefficient can be correlated with scattering center density in the bulk material.

As expected, the alkaline earth fluorides are considerably easier to cast than the alkali halides because of their more favorable mechanical

and thermal properties and smaller volume contraction on solidifying. Castings up to six inches in diameter by about one-half inch thick have been successfully fabricated. Chemical analysis indicates that the purity of the castings is equivalent to that of the starting materials.

Preliminary hot forgings of single crystal CaF_2 have been performed at temperatures near 1000°C which are sufficiently high to provide ease in forging but an attendant undesirable large grain size.

Calorimetric absorption coefficients at 5.3 μm on cast CaF_2 have been obtained in the mid 10^{-4} cm^{-1} range. Qualitative correlation between scattering center density and apparent absorption coefficients has been observed in the fluorides as was the case with the halides.

Annealing at 1000°C and slow cooling successfully removes residual stress in cast CaF_2 ingots. However, the annealing is accompanied by almost a factor of two increase in the apparent 5.3 μm absorption coefficient and a significant increase in scatter center density. These scattering centers are almost certainly caused by precipitation of impurities at the annealing temperature or by a change in the intrinsic or impurity chemistry of the fluoride with subsequent precipitation upon cooling.

PREFACE

This report was prepared by Raytheon Company, Research Division, Waltham, Massachusetts under Contract No. F19628-74-C-0148 entitled "Casting of Halide and Fluoride Alloys for Laser Windows." This work is supported by the Advanced Research Projects Agency and is monitored by the Air Force Cambridge Research Laboratories, Bedford, Mass.

At Raytheon Company the investigation is being carried out in the Materials Processing Laboratory of the Research Division. Dr. D.W. Readey is the project manager and Dr. R.T. Newberg is the principal investigator. H. Newborn, T. Wong and A. De are assisting with the material fabrication and processing. Dr. T. Kohane and T. Varitimos are performing optical absorption measurements. Dr. P. Miles is acting as a consultant to the program. This report has been given an internal number of S-1714.

TABLE OF CONTENTS

TABLE OF CONTENTS (CONT'D)

LIST OF ILLUSTRATIONS

LIST OF ILLUSTRATIONS (CONT'D)

LIST OF TABLES

1.0 INTRODUCTION

The continued progress in the design and realization of laser and optical systems, particularly that of high power infrared lasers operating in the 2 to 6 μm and 10.6 μm wavelength regions, has created the need for improved window and lens materials suitable for use in large, high-resolution optical systems. Specifically, these materials must be strong, scatter-free, and have low absorption to satisfy optical element requirements in sizes that would often be difficult to fabricate from a common optical material such as glass. Thus, to make large, strong, high-quality optical elements from the better infrared transmitting materials such as the alkali halides and alkaline earth fluorides is indeed a formidable task.

Until recently, only pure, single-crystal and hot-pressed polycrystalline optical elements of these materials have been available. Neither the process of single-crystal growth nor that of hot pressing can be easily scaled to larger sizes. Furthermore, pure single crystals are not strong enough and hot pressed material does not have low enough scatter and absorption to allow the fabrication of large, high quality infrared optical elements.

We have been actively engaged in a program whose primary goal has been to evaluate fusion casting as a fabrication technique for polycrystalline infrared window materials. Fusion casting is an attractive process in that it offers the possibility of obtaining dense, scatter-free material and can be easily scaled to larger sizes.

The effort on this program was directed to the alkali halides with the objectives of investigating the effects of grain size and alloying on the mechanical and optical properties of cast material. Emphasis was placed on obtaining high yield strengths and low 10.6 μm absorption with KCl-$SrCl_2$ alloys as a function of alloy content, grain size and heat treatment. The major achievements were the fabrication on eight-inch diameter,directionally-solidified castings with yield strengths typically around 4000 psi,with some as high as 9000 psi in certain alloys; and optical absorption coefficients in the mid 10^{-4} cm^{-1} range for these

same alloys. These results have been extremely encouraging, yet a major problem with high residual stress in cast halides still remains.

In the proposed program, we will address ourselves to the residual stress problem. The characterization of KCl-$SrCl_2$ alloys will also be completed, thus allowing us to completely demonstrate the feasibility of strengthening and casting alkali halides while maintaining their low 10.6 μm optical absorption. It is expected that this phase of the effort will be completed during the first six months of the present program.

The bulk of the program is directed to casting alkaline earth fluoride alloys for optical elements in the 2 to 6 μm region. Many of the properties of the alkaline earth fluorides such as thermal conductivity, strength, thermal expansion coefficients, etc., make them far superior to the alkali halides for fabrication by casting. The experience we have had with these materials indicates that this is indeed the case. We are specifically investigating the feasibility of fusion casting alkaline earth fluorides by measuring the optical and mechanical properties of the cast material. The effects of alloy additions and heat treatment on mechanical and optical properties are also being investigated and an optimum composition and fabrication process will be developed.

2.0 ALKALI HALIDES

2.1 Initial Program Objectives

The program previously funded under AFCRL Contract No. F19628-72-C-0307 was originally proposed to develop stronger forms of both the alkali halides and the alkaline earth fluorides and to investigate the feasibility of their fabrication by fusion casting. Because of the intense interest in the alkali halides for 10.6 μm window applications, the entire effort was devoted to the halides. All of the results of that program are presented in detail elsewhere[1-3] and will not be repeated here. In the present program, a few extensions of this work are being made in order to complete the earlier results and to solve some of the major remaining problems with the halides.

2.2 Completion of Halide Work

The comparison of yield strengths obtained with KCl-$SrCl_2$ alloys as single crystals, forged crystals, as-cast material, and forged cast alloys is being completed. In conjunction with this, the effect of increased $SrCl_2$ content on grain size of as-cast alloys is being investigated. In addition, the concentration profile of $SrCl_2$ through the ingot cross section is being more firmly established.

The effects of in situ and prepurification of the starting materials with reactive gases such as CCl_4 are being determined for cast ingots. The main goal here is to ensure that grain boundaries are not a source of absorption centers and to obtain even lower absorption coefficients than those already achieved.

Finally, to characterize the precipitation process and its effects on optical properties, the measurement of scattering as a function of wavelength for alloys of different $SrCl_2$ contents and heat treatments is being completed.

2.3 Residual Stress

The most severe remaining problem with the cast halide alloys is that of the high residual stresses found in the ingots as shown in Fig. 2-1. These stresses are high enough to cause cracking in some cases, and have led to the development of cracking during subsequent cutting and polishing in others. These stresses are doubtlessly introduced during the cooling cycle due to temperature gradients within the ingot while some regions are more plastic than others. These temperature gradients can be decreased by decreasing the overall cooling rate. To estimate how low a cooling rate might be necessary for KCl, consider two regions in the ingot separated by a distance d, in a constant temperature gradient $\Delta T/d$. If no plastic deformation takes place, then the stress in each (one in compression and the other in tension) is approximately:

$$\sigma = \frac{\alpha E \Delta T}{2d} \tag{2.1}$$

where α is the thermal expansion coefficient and E is Young's modulus. The heat flux out of the ingot, $\dot{q}$, is

$$\dot{q} = kA \frac{\Delta T}{d} \tag{2.2}$$

where k is the thermal conductivity and A is the area through which the heat is being conducted. The rate of change in the average temperature of the ingot or the cooling rate, r, is given by:

$$r = \frac{\dot{q}}{\rho C_p V} \tag{2.3}$$

where ρ is the density, C_p the specific heat and V the volume ($V = Ad$ roughly). Combining the first and third equations we obtain

$$r \cong \frac{2k\sigma}{\alpha E \rho C_p d} \tag{2.4}$$

To insure that plastic flow does not take place, the cooling rate must be such that the yield point at any temperature is not exceeded. If we assume

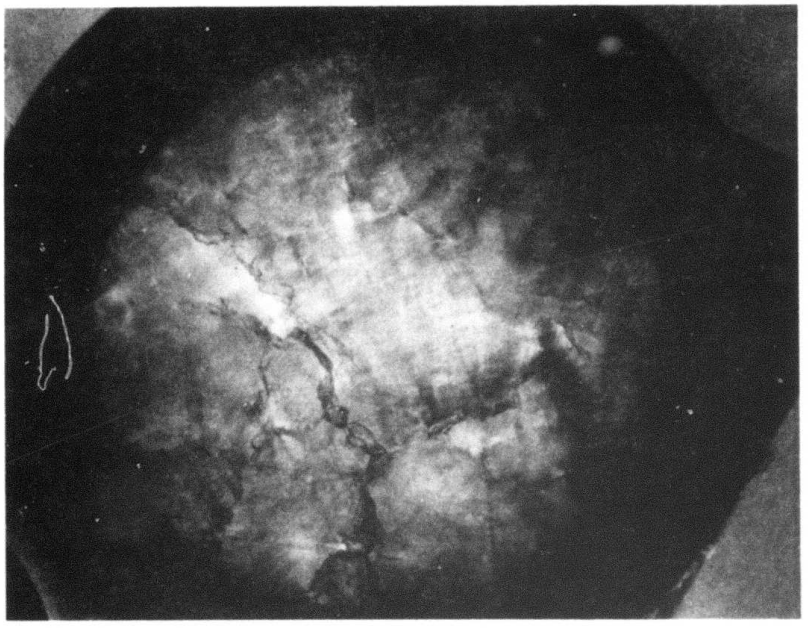

Fig. 2-1 Strain Pattern of Casting NPC-15 (200 ppm nominal $SrCl_2$) as Viewed Through Crossed Polarizers. Three inch diameter sample.

that stresses must not exceed approximately 100 psi, and all the heat is being extracted from the bottom of a one-inch-thick casting, then the cooling rate must not exceed 100°C/hr for KCl. In cylindrical castings, some heat is extracted from the mold walls which also produces a radial temperature gradient over distances as large as 4 inches in our large ingots. If this is the case, the cooling rate should not exceed 25°C/hr. This also implies that temperature gradients due to nonuniform heating or cooling should be no larger than one degree per inch.

Clearly, in order to prevent the establishment of these residual stresses, the cooling rate and temperature uniformity of the casting must be carefully controlled. Since this may be difficult to accomplish in practice, we are also investigating the effectiveness of post fabrication annealing to remove residual stresses.

3.0 OPTICAL PROPERTIES OF FLUORIDES

3.1 Infrared Absorption

The basic argument in favor of the fluorides as the materials most suitable for high-power laser windows in the 2-6 μm range are already well established, and relate directly to the predicted "failure" mechanisms of a window or lens subjected to high-power radiation. Deterioration is caused first by thermal distortion of the system elements and results in changes in focal length and aberration effects. At higher power levels, plastic flow, melting, and fracture of the optical elements will take place to give irreversible changes in the system. Uncontrolled power reflection from distorted or broken elements can then lead to damage of components not considered part of the high-power optical path itself.

The specific case of distortion and fracture of window elements has been considered in some detail, both in these laboratories[4-6] and at Rand Corporation.[7,8] The figures of merit which have been derived to characterize candidate window materials are summarized in Table 3-1. Regardless of the mode of operation, pulsed or CW, or of the cooling configuration, the materials factor governing distortional failure is $(\beta\chi)^{-1}$ or $(\beta_s\chi)^{-1}$, and the factor governing resistance to failure by fracture is $\sigma/\alpha\beta E$ or $\sigma/\alpha\beta_s E$, for bulk loss (β) and surface loss (β_s) respectively. The alkaline earth fluorides have the double advantage of an extremely low predicted loss coefficient β, and the lowest optical distortion parameter (χ) of all the various ionic and partially covalent semiconductor compounds presently under consideration for laser windows.

The fundamental, unavoidable optical absorption mechanism operative in fluorides at wavelengths near 6 μm is the excitation of lattice vibrations, primarily as a multiphonon process; that is, the simultaneous excitation of several lattice modes, together with various combinations of mode excitation and de-excitations.

In the past, quantitative analysis of multiphonon absorptions has been relatively useless in predicting the actual level of absorption. Our

TABLE 3-1a

Figures of Merit for Bulk Absorption Only

		Fracture		Optical Distortion at Wavelength (λ)	
cw	Edge-cooled	$\left(\frac{\sigma_c}{\alpha\beta E}\right) \cdot K$	watts	$\left(\frac{\lambda}{\beta\chi}\right) \cdot \frac{K}{R}$	watts
	Face-cooled	$\left(\frac{\sigma_c}{\alpha\beta E}\right) \cdot (K + .. h_S^* R)$	"	$\left(\frac{\lambda}{\beta\chi}\right) \cdot \left(\frac{K}{R} + .. h_S^*\right)$	"
	Pulsed	$\left(\frac{\sigma_c}{\alpha\beta E}\right) \cdot \left(\frac{CR^2}{t}\right)$	"	$\left(\frac{\lambda}{\beta\chi}\right) \cdot \left(\frac{CR}{t}\right)$	"

TABLE 3-1b

Figures of Merit for Surface Absorption Only

		Fracture		Optical Distortion	
cw	Edge-cooled	$\left(\frac{\sigma_c}{\alpha\beta_s E}\right) \cdot KR$	watts	$\left(\frac{\lambda}{\beta_s\chi}\right) \cdot K$	watts
	Face-cooled	$\left(\frac{\sigma_c}{\alpha\beta_s E}\right) \cdot KR + .. h_S^* R^2)$	"	$\left(\frac{\lambda}{\beta_s\chi}\right) \cdot (K + .. h_S^* R)$	"
	Pulsed	$\left(\frac{\sigma_c}{\alpha\beta_s E}\right) \cdot \left(\frac{CR^3}{t}\right)$	"	$\left(\frac{\lambda}{\beta_s\chi}\right) \cdot \left(\frac{CR^2}{t}\right)$	"

... this table:

σ_c is the critical failure stress

α is the expansion coefficient

β is the bulk absorption coefficient

β_s is the surface absorption coefficient

E is the Young's modulus

K is the thermal conductivity

h_S^* is the surface heat transfer coefficient

R is the window radius

C is the specific heat

t is the pulse length

χ is an optical distortion parameter

$$= \frac{dn}{dT} + (1+\nu)\alpha(n-1) + \frac{1}{2} n^3 \alpha E \langle\pi\rangle$$

where

n = index of refraction

ν = Poisson's ratio

$\langle\pi\rangle$ = an averaged stress-optic coefficient

experiments on a number of fluorides and other halides, however, have shown that there exists a characteristic wavelength (λ) dependence for the absorption coefficient, namely

$$\beta = \beta_0 \exp - \left(\frac{\lambda_0}{\lambda}\right) = \beta_0 \exp - \left(\frac{\bar{\nu}}{\bar{\nu}_0}\right) \qquad (3.1)$$

where β_0 lies in the range 10^4 - 10^5 cm^{-1} and λ_0 ($= 1/\bar{\nu}_0$) is related to the free space wavelength associated with the zone center-longitudinal vibrational mode. Experimentally, the value of λ_0 is approximately 4.5 times the mode wavelength. The actual values that have been derived for a number of IR materials are listed in Table 3-2.

TABLE 3-2

EXTRAPOLATED MULTIPHONON LOSS FACTOR FOR CANDIDATE MATERIALS

Material	6 μm	5.3 μm	3.8 μm	2.8 μm	2 μm
BaF_2	$\approx 10^{-5}$	$\approx 10^{-6}$	$< 10^{-6}$	$< 10^{-6}$	$< 10^{-6}$
SrF_2	2×10^{-4}	$\approx 10^{-5}$	$< 10^{-6}$	$< 10^{-6}$	$< 10^{-6}$
CaF_2	1.8×10^{-3}	3×10^{-4}	$< 10^{-6}$	$< 10^{-6}$	$< 10^{-6}$
MgF_2	8×10^{-2}	1.2×10^{-2}	6.5×10^{-5}	$< 10^{-6}$	$< 10^{-6}$
MgO	0.2	2×10^{-2}	0.6×10^{-4}	$\approx 10^{-6}$	$< 10^{-6}$

Excess loss { Initial Requirements ||||| ; Stringent Requirements ≡≡≡

From the data in Table 3-2, it is obvious that, as a group, the fluorides, in pure form, are capable of satisfying the requirements of $\beta < 10^{-4}$ cm^{-1} at the important laser wavelengths, 5.3 μm (CO), 3.8 μm (DF) and 2.8 μm (HF).

3.2 Optical Scattering

The optical quality of an otherwise transparent material free from absorptive loss, and with perfect optical surfaces, will be determined by

optical inhomogeneity produced either by built-in strain, by density changes in composites where there are two or more components, by porosity, or by refractive-index discontinuities at the boundaries of noncubic crystallites.

A polycrystalline material with cubic crystal symmetry, such as an alkaline earth fluoride, will not scatter if it is 100 percent dense, with no pores. The crystalline boundaries, while recognized as discontinuities at X-ray wavelengths, will be essentially invisible at all wavelengths greater than 10Å notwithstanding the size of the crystallites. Pores or inclusions smaller than 0.1 μm will produce wide-angle scatter that depends on wavelength, decreasing as the wavelength increases approximately as $1/\lambda^4$ in the visible and IR region. Larger pores or inclusions will scatter in a manner depending on their shape and orientation to a degree that will decrease as $1/\lambda^2$ in the visible and near-IR and eventually as $1/\lambda^4$ at longer wavelengths.

In practice, even single crystals in general show the presence of discrete scatter centers throughout the bulk. Their nature is unknown, but oxide, sulphate or carbonate precipitates are likely candidates. The likelihood of aggregation of similar impurities in polycrystalline materials implies that particular attention must be paid to prepurification of starting materials and heat treatment procedures.

4.0 MECHANICAL PROPERTIES AND STRENGTHENING OF ALKALINE EARTH FLUORIDES

4.1 Introduction

A primary objective of this program is to fabricate high-strength alkaline earth fluorides using common metallurgical strengthening and fabrication techniques,keeping in mind the feasibility and cost of scale-up to the desired size. The effort on strengthening and fabrication of alkali halide materials for the 10.6 μm laser window has demonstrated the feasibility and applicability of these strengthening and fabrication techniques. In the case of the alkali halides, increases in yield and fracture strengths of well over an order of magnitude have been shown to be possible.[1]

On the other hand, background information, available for a large portion of the alkali halide work, is lacking for the alkaline earth fluorides. Therefore, discussion of hardening and fabrication techniques for these materials must rely on far less available experimental data. However, the alkaline earth fluorides, as pure materials, are significantly stronger than the halides,and the incremental increases in strength required for them to be useful window materials are proportionately less. In this context we will discuss various possible strengthening techniques for the alkaline earth fluorides, keeping in mind their unique chemical and crystallographic properties. Specifically, the effects of grain size, solid-solution alloying, and precipitation hardening will be discussed as strengthening mechanisms, since we propose these as the techniques for producing strong polycrystalline high-power laser windows.

4.2 Strengthening Mechanisms

4.2.1 Grain size effects

The efficacy of grain size reduction in increasing the yield strength of the alkali halides is now fairly well documented. According to the Von Mises criterion, for a randomly oriented polycrystalline solid to deform plastically, it must be presumed that each grain is capable of undergoing

perfectly general strain in order to conform to the distortion of its neighbors. At least five independent slip systems are required to satisfy this general requirement. Even in those materials in which five independent slip systems are operative, dislocations pile up at grain boundaries and restrict macroscopic plasticity. It can be shown that this leads to an inverse square root ($d^{-\frac{1}{2}}$) dependence of yield strength on grain size, the so-called Hall-Petch relationship. This relationship is observed for many ductile materials and has been demonstrated to be true for polycrystalline KCl.[9]

In the fluorite structure materials CaF_2, SrF_2, and BaF_2, the most active slip system at low temperature is $\{100\}\ \langle 1\bar{1}0\rangle$ [10-12] which gives only three independent systems.[13] In fact, even this system is relatively inoperative in CaF_2 at room temperature, and both single and polycrystals of this material fail by brittle fracture with essentially no macroscopic yielding. However, above about 200°C the two $\{110\}\ \langle 1\bar{1}0\rangle$ systems become active in CaF_2 and, along with the three $\{100\}\ \langle 1\bar{1}0\rangle$ systems, give the necessary five independent systems. Thus, polycrystalline CaF_2 at elevated temperatures does deform plastically.[14] Presumably SrF_2 and BaF_2, also having the fluorite crystal structure, behave similarly at elevated temperatures. In fact, they are probably more plastic than CaF_2 because of their smaller ionic character, as indicated by their larger lattice parameters. However, little information is available on the plastic behavior of these materials except on a microscopic scale.[11, 12]

At temperatures near 300°K, most of the alkaline earth fluorides, both single and polycrystals, fail by brittle fracture. Fracture in polycrystalline materials which undergo only a small amount of plastic deformation as single crystals can be initiated by crack nuclei produced by deformation.[15-18] Analysis of this mechanism leads to an inverse square root dependence of fracture strength on grain size. Since CaF_2, SrF_2 and BaF_2 all exhibit at least microplastic behavior at room temperature, it might be expected that their fracture strength will follow a Petch relationship. Therefore, fracture strength of the alkaline earth halides should increase as the grain size decreases and should also increase

if dislocation motion is restricted by solid solution or precipitation hardening. This, of course, assumes adequate surface preparation so that surface flaws are not strength limiting. At present, whether the existence of surface flaws or microplasticity is the strength limiting factor is not known.

4.2.2 Solid-solution strengthening

4.2.2.1 General

If fracture in these materials is nucleated by a dislocation pile-up mechanism, solid solution hardening will increase the fracture strength simply because it impedes dislocation motion. Therefore, as part of this program, we are investigating solid-solution alloying as a means of increasing the strength of alkaline earth fluorides. In fact, because of the divalent alkaline earth ions, these materials offer some interesting possibilities for solid-solution effects not available in the alkali halides.

4.2.2.2 Divalent additions

As solid solutions are made between divalent alkaline earth fluorides, the resistance to plastic flow will increase simply because of the spherical distortion of the lattice caused by ions of slightly different size impeding dislocation motion. In the alkali halides, we and others have obtained increases in yield strength of KCl-KBr alloys from 250 psi to over 2000 psi near the 50-50 composition. However, with such concentrated solid solutions, a significant decrease in thermal conductivity, coupled with the considerable decrease in plasticity, makes the material extremely thermal-shock sensitive and almost impossible to work with. Since a comparable decrease in thermal conductivity would be expected in the alkaline earth fluorides with questionable improvement in strength, the investigation of solid solutions of the divalent fluorides does not offer much promise of improved materials.

4.2.2.3 Aliovalent additions

In contrast to monovalent impurities in the alkali halides, divalent impurities produce very significant increases in yield stresses at very low

concentrations. In fact, the yield strength of KCl single crystals, for example, can be increased by a factor of over twenty by the addition of a few hundred parts per million of Sr^{2+}.[1,3] This difference in behavior between monovalent and divalent impurities in KCl has been observed for a number of different impurities.[19] Here again, virtually no information exists on the effects of aliovalent impurities on the alkaline earth fluorides. However, an increase in oxygen content of only 40 ppm in CaF_2 single crystals has been observed to decrease dislocation velocity by almost an order of magnitude.[20] Also, one of the few pieces of data on fluorides indicates that small additions of Nd^{3+} to CaF_2 can significantly decrease dislocation mobility.[21]

Several explanations of the strong hardening effect of aliovalent impurities have been proposed. Several possible mechanisms have been suggested, based on impurity-defect dipole pairs interacting with dislocation motion. One mechanism in which these dipoles can impede dislocation motion is by the tetragonal distortion produced along the dipole axis.[22] In the case of additions such as YF_3 and other rare earths in CaF_2, the extra fluorine goes into an interstitial site in the fluorite lattice.[23] The interstitial F^- coupled with the Y^{3+} on a Ca^{2+} site forms a dipole pair which produces a nonspherical lattice distortion.[24] This distortion would be expected to be as effective as divalent impurity-vacancy pairs are in the alkali halides.

The alkaline earth fluorides also offer greater flexibility than the alkali halides in that both trivalent and monovalent impurity additions may be used. The possibility exists in the alkaline earth fluorides for paired substitutions such as NaF and YF_3, together in CaF_2. In this case, no lattice defects should form and the Na^+ and Y^{3+} should produce a nearest cation neighbor pair producing the nonspherical lattice distortion and attendant hardening discussed above. Furthermore, the solubility of such a paired substitution should be much greater, permitting the possibility of greater hardening.

4.3 Systems Being Investigated

The mechanical behavior of the alkaline earth fluorides has been investigated only to a very limited extent. Because the amount of plasticity exhibited by these materials is uncertain and because of the effect of plasticity on strength, the efficacy of various strengthening techniques is questionable. In fact, the effects of grain size and alloying on mechanical properties has not been studied in these materials at all. Furthermore, only limited phase equilibria exist for potential alloy systems of these materials, making the choice of materials systems even more difficult. Despite these difficulties, and in order to develop materials with properties and processing techniques amenable to scale up, a few systems can be specified based on our experience with the alkali halides and the qualifying factors discussed above.

Table 4-1 lists some pertinent properties of the alkaline earth fluorides. As pointed out in our earlier discussion, these data indicate that only SrF_2 and BaF_2 meet the requisite low-optical-absorption requirements out to six micrometers. However, SrF_2 is clearly preferable to BaF_2 because it has a much lower solubility and higher intrinsic hardness. The properties of CaF_2 are similar to those of SrF_2 with the exceptions of the higher absorption coefficient and lower solubility of CaF_2. Furthermore, CaF_2 and SrF_2 have lattice parameters and cation radii within fifteen percent of each other and available phase equilibria indicate, as might be expected, that they form a continuous series of solid solutions.[25] Due to the similarities in these materials, a somewhat better understanding of the mechanical properties of CaF_2,[14] and greater availability of phase equilibria data on CaF_2-based systems, the initial efforts are being directed to CaF_2 and, where successful, will be transferred to the desired SrF_2 system. For example, the effects of paired substitutions of YF_3 and NaF on the properties of CaF_2 are being determined. If, as expected, increases in mechanical properties are obtained, similar substitutions will be tried with SrF_2.

TABLE 4-1

PROPERTIES OF ALKALINE EARTH FLUORIDES*

	MgF_2	CaF_2	SrF_2	BaF_2
Melting point (°C)	1312	1408	1400	1320
Crystal structure	tetragonal, (SnO_2)	cubic	cubic, (CaF_2)	cubic, (CaF_2)
Lattice parameter (Å)	$a_0 = 4.623$ $C_0 = 3.052$	5.46	5.800	6.200
Cation radius (Å)	0.66	0.99	1.13	1.34
Minimum optical absorption at 5.3μ m (cm^{-1})	1.2×10^{-2}	3×10^{-4}	$\sim 10^{-5}$	$\sim 10^{-6}$
Thermal expansion coefficient (10^{-6} °C^{-1})	$a_{\perp} = 11.89$ $a_{\parallel} = 16.21$	18.5	17.5	18.1
Thermal conductivity (cgs)	0.0360	0.0237	0.0239	0.0287
Elastic modulus (10^6 psi)	16.6 - 24.5	14.2 - 21.0	14.5	9.6
Hardness (Knoop)	415	120 - 163	130	65 - 82
Water solubility (μg/ml H_2O)	76	16	110	1700
Density (g/cc)	3.177	3.181	4.20	4.886

* Room temperature and single crystal data from a number of sources, primarily C.S. Sahagian and C. A. Pitha, "Compendium on High Power Infrared Laser Window Materials," Rept. AFCRL-72-0170, March 9, 1972.

5.0 FABRICATION PROCESSES FOR FLUORIDES

5.1 Casting

One of the primary goals of this program is to investigate the feasibility of fusion casting as a fabrication technique for optical materials. As we have shown with the alkali halides, casting is advantageous because it is a conceptually simple technique which produces high-density materials with the potential of easy scale up. Of course, problems with casting do exist; a major one is the formation of voids, cracking and residual stresses brought about by the large thermal expansion coefficients, poor thermal conductivities and large volume contractions on freezing of ionic compounds.

For the alkaline earth fluorides, the situation is much more easily controlled since they have smaller expansion coefficients, higher thermal conductivities and smaller volume contractions on freezing than the alkali halides. For example, Fig 5-1 compares the volume contraction of SrF_2 (a typical alkaline earth fluoride) with those of KCl (a typical alkali halide), aluminum and silver relative to their respective melting points, T_m. As might be expected, the volume contractions of the fluorides during freezing are considerably less than the alkali halides,yet larger than metals. On the other hand, the volume contraction for the fluoride in the solid during cooling is more similar to the alkali halides. Nevertheless, the volume contraction still strongly suggests that the alkaline earth fluorides must be directionally solidified, leaving the free liquid to absorb the volume contraction just as with the alkali halides. In any event, our experience with both the halides and fluorides indicates that the fluorides are considerably easier to fabricate by casting than the halides.

5.2 Hot Forging

As we have done with the alkali halides, we propose to investigate hot-forging of the fluoride alloys as a means to improve microstructure and mechanical properties. By a proper sequence of deformation and recrystallization heat treatments, it is expected that the grain size can be refined in order to obtain the full benefit of the strengthening behavior of small grain sizes.

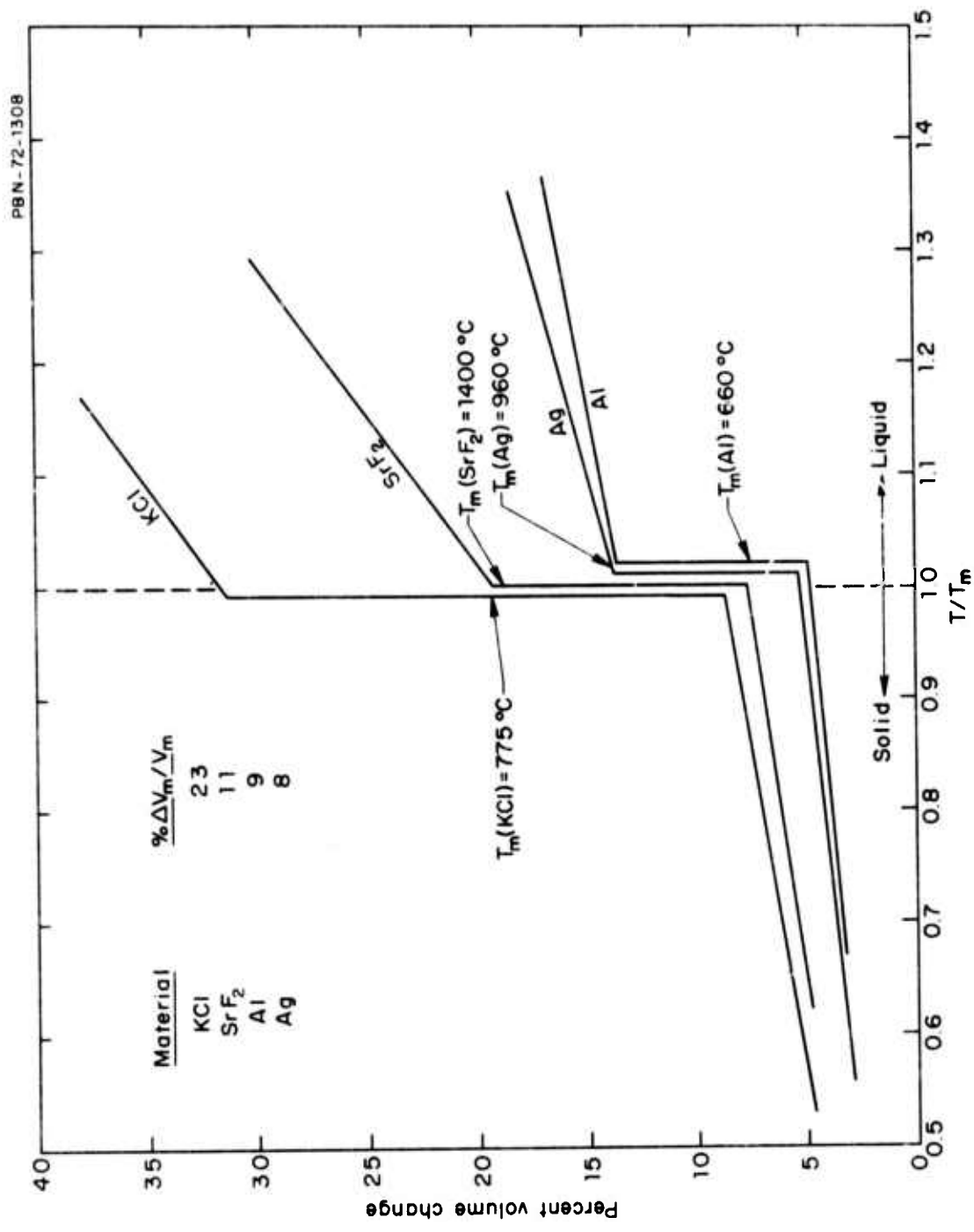

Fig. 5-1 Comparison of the Volume Contraction of SrF_2 Near the Melting Point, T_m, with Those of KCl, Aluminum and Silver.

Hot forging of KCl, both in our own and other laboratories, has produced materials with uniform grain sizes below ten micrometers and yield strengths in excess of 2000 psi. One of the main difficulties with the technique is that the temperature and stress cycles must be carefully controlled to prevent secondary grain growth which may result in, at most, very large-grained material, or, at least, a material having a duplex microstructure. However, the time-temperature cycle can be properly controlled to give a uniform, fine-grain-size microstructure which produces the high yield point.

Because of their higher melting points, different slip systems, and different slip-system temperature dependencies, the hot-forging parameters for the alkaline earth fluorides are doubtlessly quite different from those of the alkali halides. Preliminary experiments in our laboratory indicate this to be the case.

5.3 Starting Materials and Purification

All three types of possible impurities, dissolved anion and cation impurities and second phase particles, are more likely to occur in the alkaline earth fluorides than in the alkali halides because of the higher melting points of the fluorides. Cation impurities in commercially-available starting material may not be particularly deleterious to optical properties at levels of 1000 parts per million level or less if they are in solid solution as fluorides, unless, of course, the particular fluoride has an extremely high absorption coefficient. For example, magnesium would be expected to be a common impurity in CaF_2. A Mg concentration of 1000 ppm would be expected to contribute only about $\beta \cong 10^{-5}$ cm^{-1} at 5 μm wavelength since the absorption coefficient of MgF_2 is about 10^{-2} at this region. If cations dissolved as fluorides are a problem, then getting rid of them by processes such as zone refining is more difficult because of the relatively high melting point of the fluorides. Impurity cation removal is probably more effectively handled by wet chemical processing of the fluorides or of their precursor chemicals. Therefore, in this program, we are initially investigating the suitability of various

commercially-available starting chemicals, relating cation impurity content with optical properties and attempting to determine the minimal level of purity necessary to satisfy properties.

Doubtlessly, the anion impurities will be much more troublesome, particularly oxygen. First, at low levels, oxygen can combine with the impurity cations to form precipitates, or impurity-oxygen pairs, or clusters which will degrade optical properties considerably. At higher oxygen or water vapor levels, reactions typified by:

$$CaF_2 + H_2O_{(g)} \rightleftharpoons CaO + 2HF_{(g)} \qquad (5.1)$$

are thermodynamically favorable.

If powdered starting fluorides which have been exposed to oxygen or water-vapor-containing atmospheres are used, some pretreatment or in-process treatment must be used to remove any oxides present. There have been two common techniques by which this has been accomplished. First, small additions of lead fluoride are effective if the oxide concentration is not too large, since the following reaction is favorable:

$$PbF_{2(s)} + CaO_{(s)} \rightleftharpoons CaF_2 + PbO_{(g)} \quad . \qquad (5.2)$$

Also, at the melting point of CaF_2, the vapor pressure of PbF_2 is sufficiently high so that any excess is effectively removed by evaporation. This is a relatively simple and easily used technique.

Another somewhat more difficult purification reaction is:

$$2HF_{(g)} + CaO \rightleftharpoons CaF_2 + H_2O_{(g)} \quad , \qquad (5.3)$$

since a system resistant to HF must be used. This purification reaction is most effectively carried out on powders which are then either sintered or melted to reduce surface area prior to further processing. During the initial part of this program, our efforts are concentrating on using PbF_2 and other fluorine producing scavenger materials[28] to purify the fluoride materials.

6.0 RESULTS

6.1 Alkali Halides

6.1.1 Single crystals

A number of single crystals of undoped and $SrCl_2$-doped KCl grown during the program previously funded under AFCRL Contract No. F19628-72-C-0307 were used for these studies. Starting materials for these samples had been "reagent" grade chemicals.

6.1.1.1 Hardness and precipitation

Hardness is determined with a Vickers DPH indenter and a 10 gm load mounted on a Vickers M-55 metallograph. Determined were the effects of heat treatment time and temperature on precipitation and hardness of various $SrCl_2$ doped samples of KCl. Samples were never larger than about 1.5 × 1.5 × 0.5 cm. They were first solution annealed for 15 minutes at either 650 or 700°C followed by air quenching to room temperature. Subsequent anneals were carried out at temperatures of 200, 250, 375, 425, and 500°C for times of 1/4, 1, 4, and 16 hours. Hardness was determined for each heat treatment with at least four hardness measurements for each test.

From plots of hardness versus temperature for each time of heat treatment and for each of the three $SrCl_2$ concentrations (5000 ppm, 1 and 2 percent $SrCl_2$ nominal), the temperatures at which hardness dropped to 90 percent of the solution annealed hardness value were determined. The decrease in hardness is associated with precipitation of a second phase (presumably K_2SrCl_4) as evidenced by the turbidity developed during annealing.

These results are plotted in Fig. 6-1 as a typical TTT (time, temperature, transformation) type plot.

The results show that a 10 percent drop in hardness as a result of precipitation occurs in a very short time between 350 and 450°C for

PBN-74-79

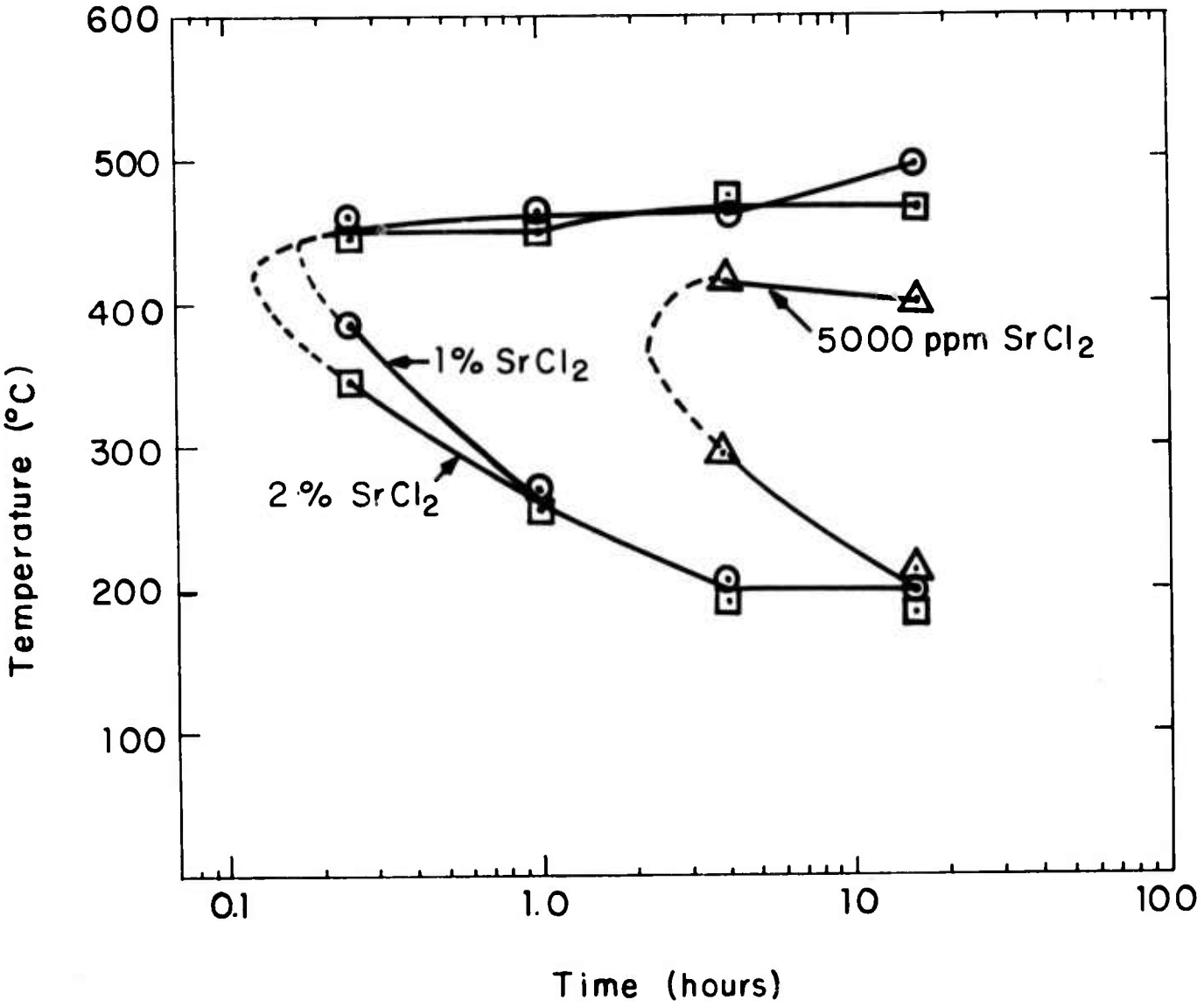

Fig. 6-1 Time-Temperature-Transformation Data for Precipitation Softening in KCl-$SrCl_2$ Alloys. The curves are for ten percent decrease in hardness.

the highest doped samples (1 and 2 percent $SrCl_2$ nominal), with very similar results for both 1 and 2 percent samples, indicating a limit has been reached. For the lower concentration (5000 ppm, $SrCl_2$ nominal), the precipitation occurs in longer times at similar temperatures, as expected. These data suggest that little difficulty should be experienced in cooling a nominal 5000 ppm (~800 ppm actual) crystal without precipitation.

6.1.1.2 Thermal conductivity

Thermal conductivity measurements were taken on samples of the variously doped $SrCl_2$-KCl samples using the thermal comparator technique. A TPRC Model 100 thermal comparator (McClure Park Corporation, West Lafayette, Indiana) was used. Sample size was approximately $1.5 \times 1.0 \times 0.5$ cm. The results were internally inconsistent and irreproducible and were found to be quite dependent on sample size, by using a few larger samples. Further work will have to be done in order to obtain good results.

6.1.2 Cast $SrCl_2$-KCl

The emphasis of casting in our two zone furnace (Figs. 6-2 and 6-3) during the first quarter of this program was directed toward the casting and annealing of fluorides. However, a number of 8-inch diameter KCl castings were made.

All castings, with the exception of two, were made from Merck "Suprapure" KCl and doped with Johnson Matthey high purity (Grade I) $SrCl_2$. The technique for casting these large pieces has been detailed previously.[1]

During this first quarter, seven high purity castings were made in a 50-ton vacuum hot press furnace (Fig. 6-4) by melting and solidifying in situ. This furnace (an all graphite system) has the capability of better vacuums than the two-zone furnace. The purpose of attempting to cast in this furnace was to evaluate whether or not the better vacuum improved

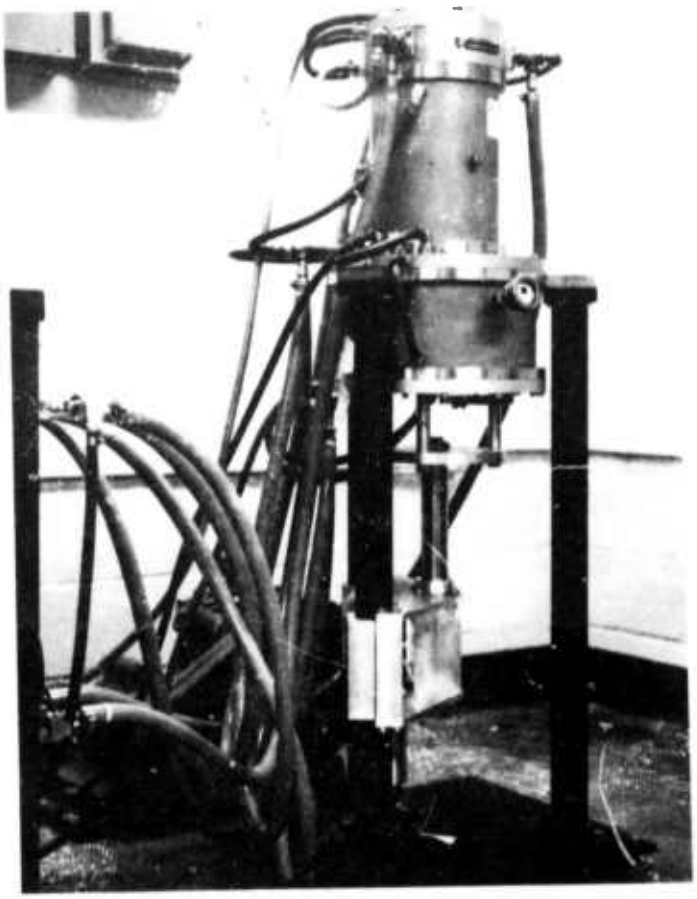

Fig. 6-2 Two Zone Casting Furnace.

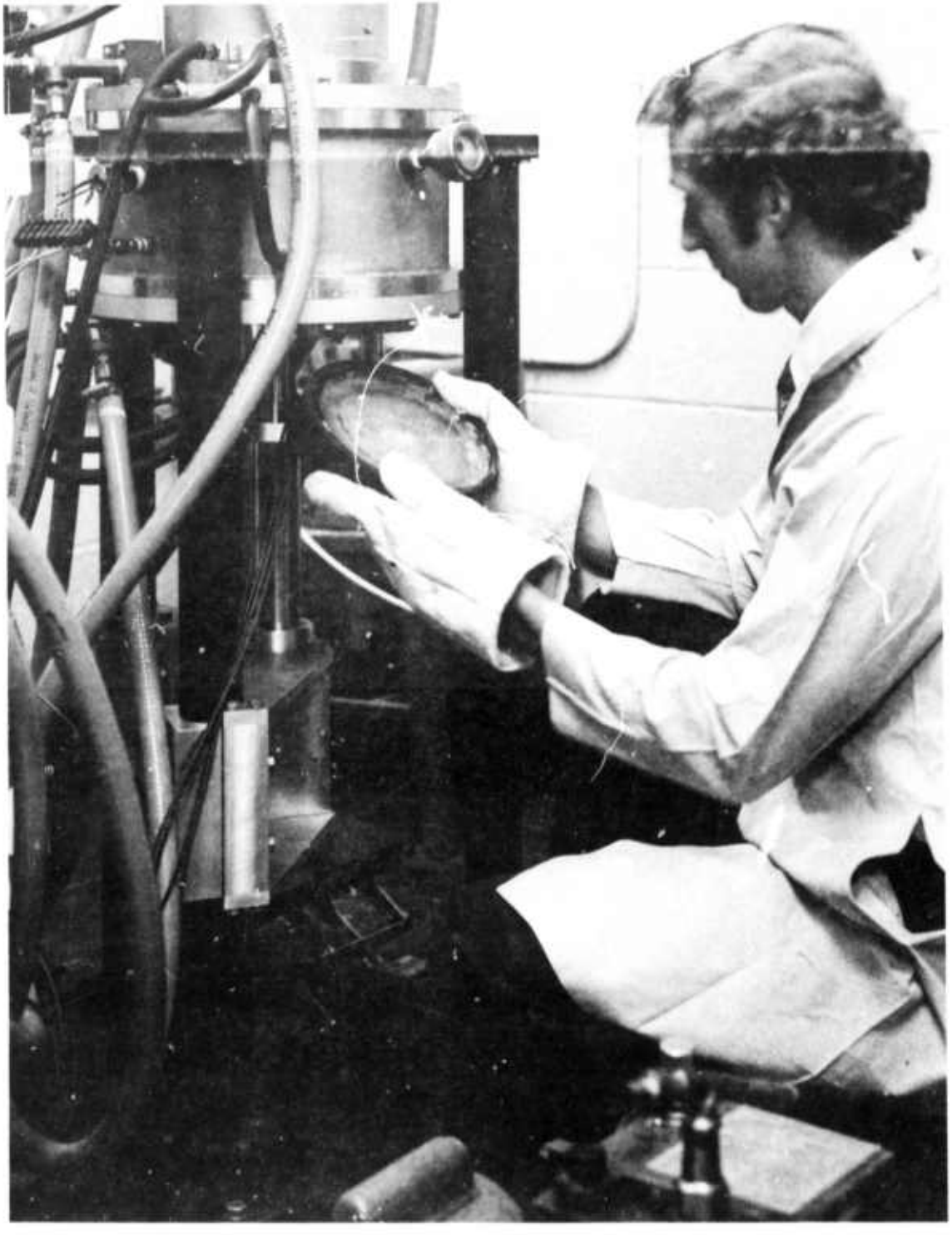

Fig. 6-3 Removal of a KCl Casting from the Two Zone Casting Furnace.

Fig. 6-4 50-Ton Vacuum Hot Press Used for Casting and Hot Forging Polycrystalline Alkaline Earth Fluorides.

the optical absorption. In the hot press furnace, a $5\frac{1}{2}$-inch diameter ATJ graphite crucible (lined with removable grafoil) with cover was used for casting. Limitations of the system were such that uniform, unidirectional solidification was difficult to achieve. However, small samples from these castings could be analyzed for optical properties which will be discussed later.

6.1.3 Strain annealing

One of the major problems in the casting of the halides is the high residual strains produced during cooling from solidification temperatures. Handling of the cooled castings has been difficult, with cracking of castings being a problem.

Significant results were found during this first quarter in successful annealing runs for the halide castings. All anneals were performed in air using a large muffle furnace. To minimize thermal gradients, each sample was loosely packed in fiberfrax insulating wool and surrounded by two-inch thick firebrick.

Successful annealing is illustrated by Figs. 6-5 and 6-6 for both pure KCl and $SrCl_2$-doped KCl samples. Figure 6-5a and 6-6a show the respective samples as cast with high residual strain as viewed through crossed polarizers. Figures 6-5b and 6-6b show the same two samples after the successful annealing treatment of 10 hours at 600°C followed by cooling at 10°C per hour to room temperature.

As a result of the success in our strain annealing procedure, several of the large-diameter castings were similarly annealed successfully and sent out for optical polishing. However, difficulty was experienced and the specimens cracked during a grinding procedure. Upon polishing, further cracking occurred (perhaps due to strains built up during grinding). It is evident that even as annealed, the castings must be handled with great care.

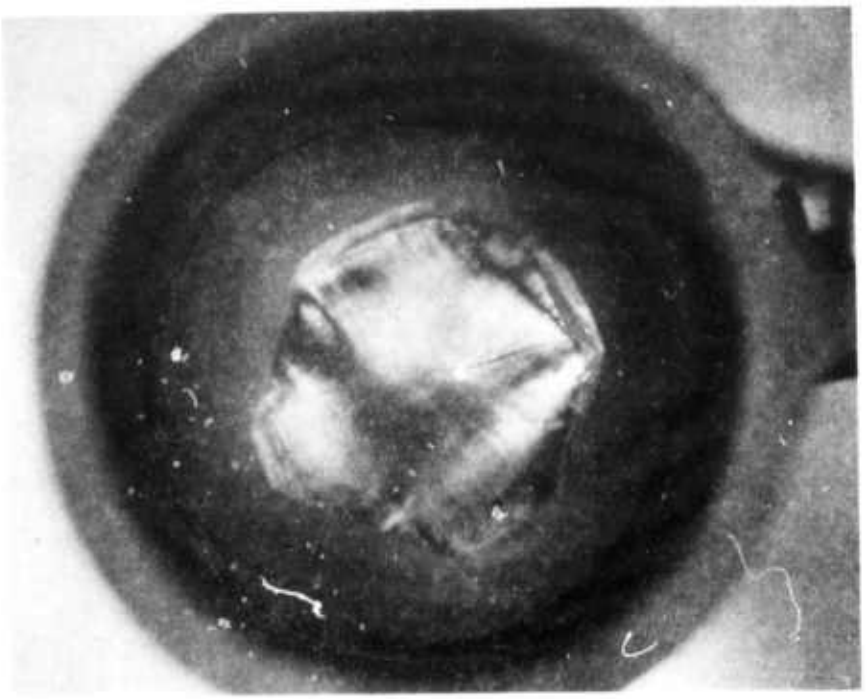

Fig. 6-5a Sample of Polycrystalline KCl As Cast. Viewed through crossed polarizers.

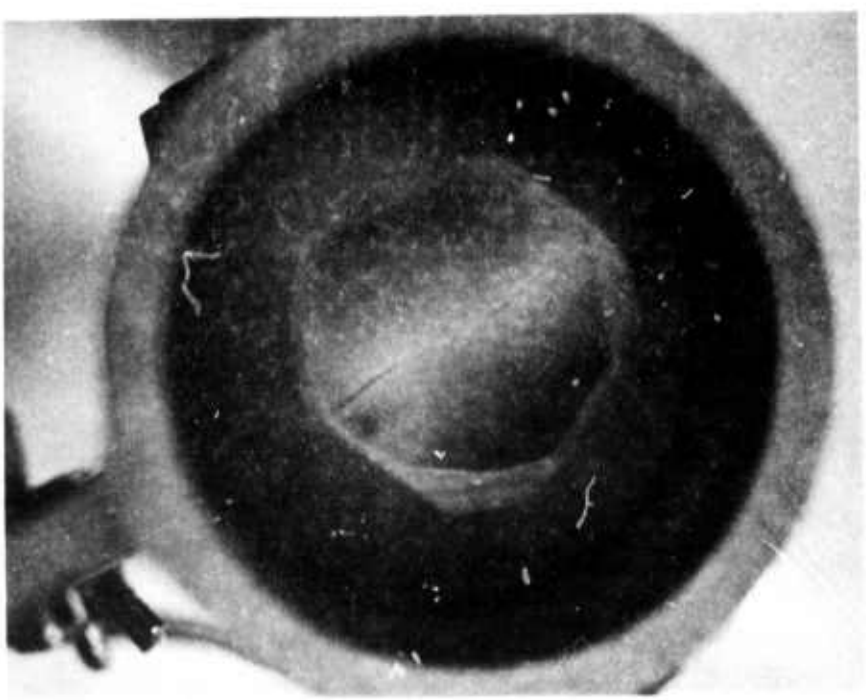

Fig. 6-5b Same Sample After Annealing at 600°C for 10 Hours then Cooled at 10°C/hr.

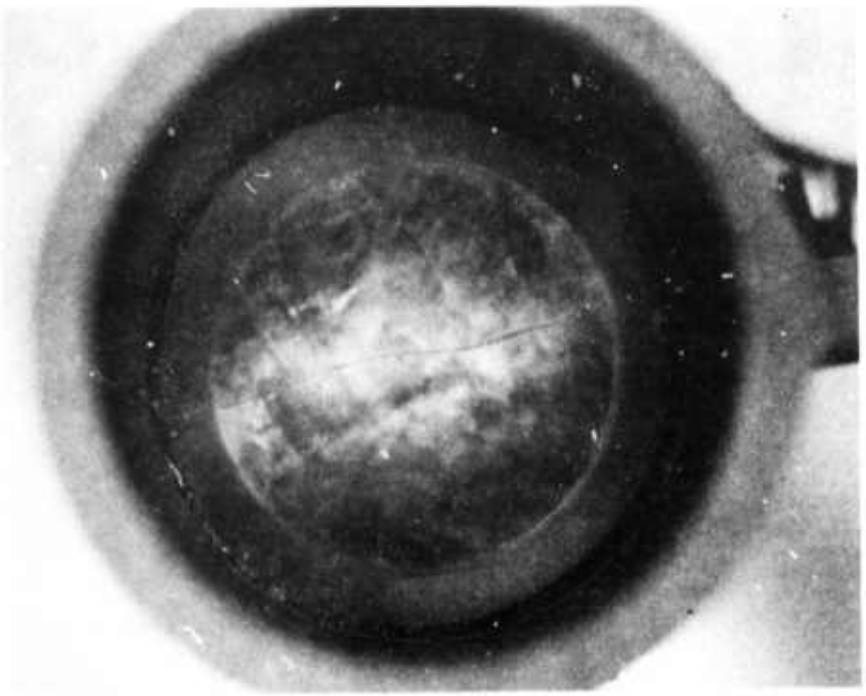

Fig. 6-6a Sample of Polycrystalline $SrCl_2$-KCl Alloy As Cast. Viewed through crossed polarizers.

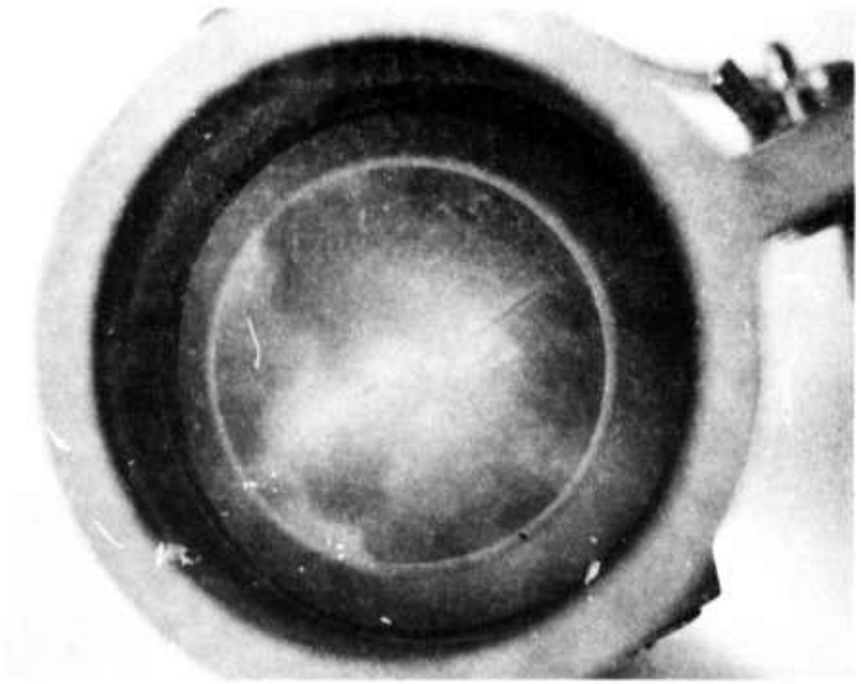

Fig. 6-6b Same After Annealing at 600°C for 10 hrs. and Cooling at 10°C/hr.

6.1.4 Optical properties

6.1.4.1 Processing effects

Two castings were made using "reagent" grade KCl that had been purified in our laboratory using a "RAP" technique. This consisted of pulling a quartz tube filled with KCl powder slowly through a furnace at 600°C. The purification consisted of bubbling dry argon through CCl_4 at room temperature and over the powdered KCl for 24 hours. That this treatment was not completely successful is shown by the IR transmission curve for a specimen from a casting of this "purified" KCl, NPC-47. Figure 6-7 shows the broad absorption band centered near 10 μm. Note however that NCO^- (2180 cm^{-1}), CO_3^{--} (1400-1500 cm^{-1}) or SO_4^{--} (1100-1200 cm^{-1}) absorption bands are not apparent, whereas for the unpurified "reagent" grade castings they are observed (Fig. 6-8).

Figure 6-9 gives the IR transmission curve for a specimen cut from a large casting of "superpure" material. Note that no detectable impurity bands are present, even though the sample path length is quite long. However, the measured 10.6 μm absorption coefficient for this sample is 4.8×10^{-3} cm^{-1}. This high an apparent absorption coefficient should correspond to an absorption of about 2 percent at 10.6 μm. If this apparent absorption were caused by the broad band near 10 μm, as seen in Figs. 6-7 and 6-8, then a dip in the IR spectrum in Fig. 6-9 comparable to that in Fig. 6-7 would be expected. However, none is observed. The implications of this are discussed more completely later.

Figure 6-10 gives the IR transmission curve for a sample cut from a $5\frac{1}{2}$-inch diameter casting produced in the vacuum hot press furnace. No impurity bands are detectable and the calorimetrically measured 10.6 μm absorption coefficient for this sample is 6.3×10^{-4} cm^{-1} (uncorrected for surface loss).

Table 6-1 gives the chemical analysis for several selected castings, as well as for the Merck "Suprapur" powder from which castings NPC-22

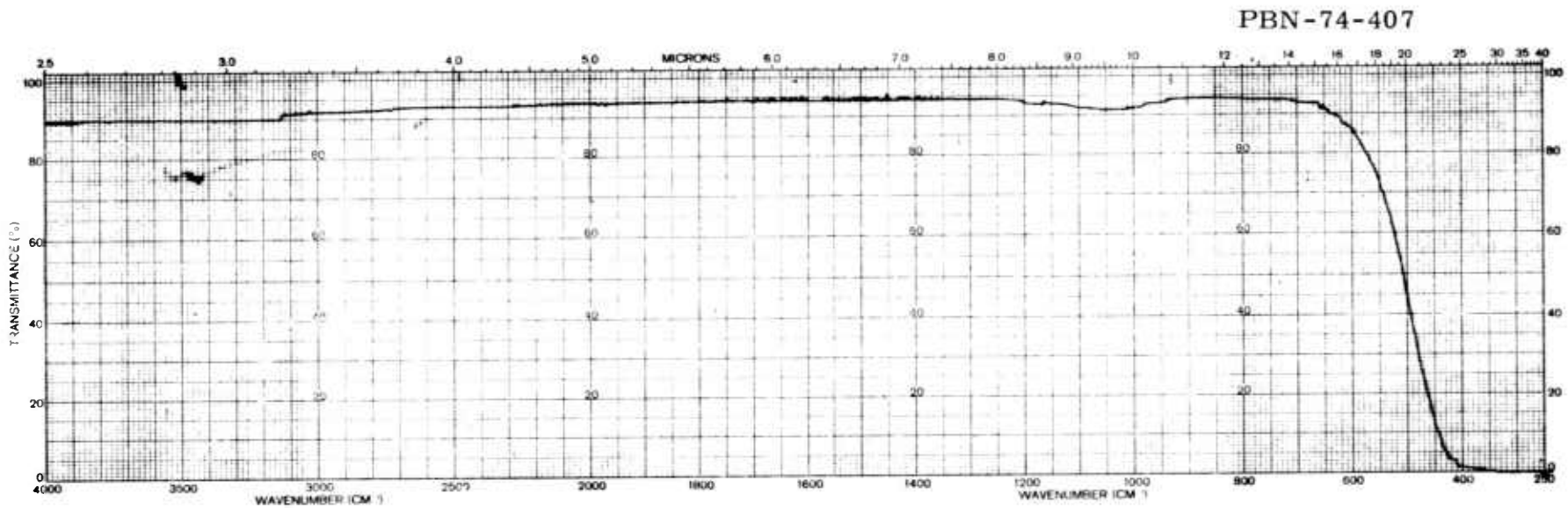

Fig. 6-7 Infrared Spectrum of Sample NPC-47 100 ppm $SrCl_2$-KCl (Purified). 1.7 cm path length.

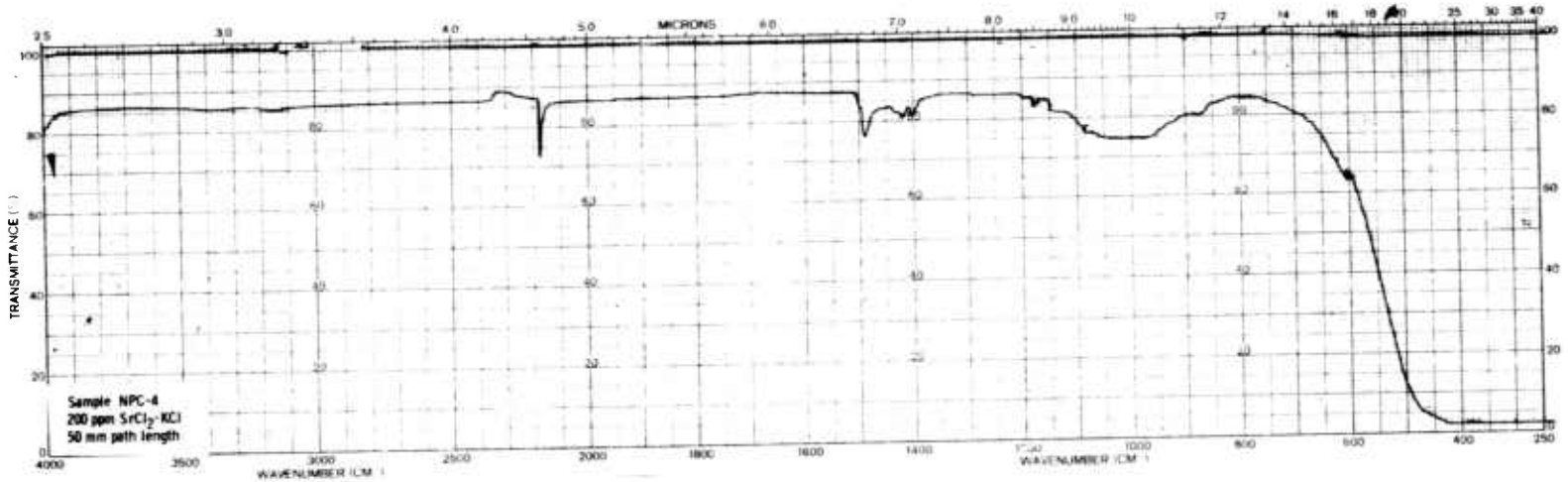

Fig. 6-8 Infrared Transmission Spectrum of Casting NPC-4 (200 ppm nominal $SrCl_2$). "Reagent" grade KCl.

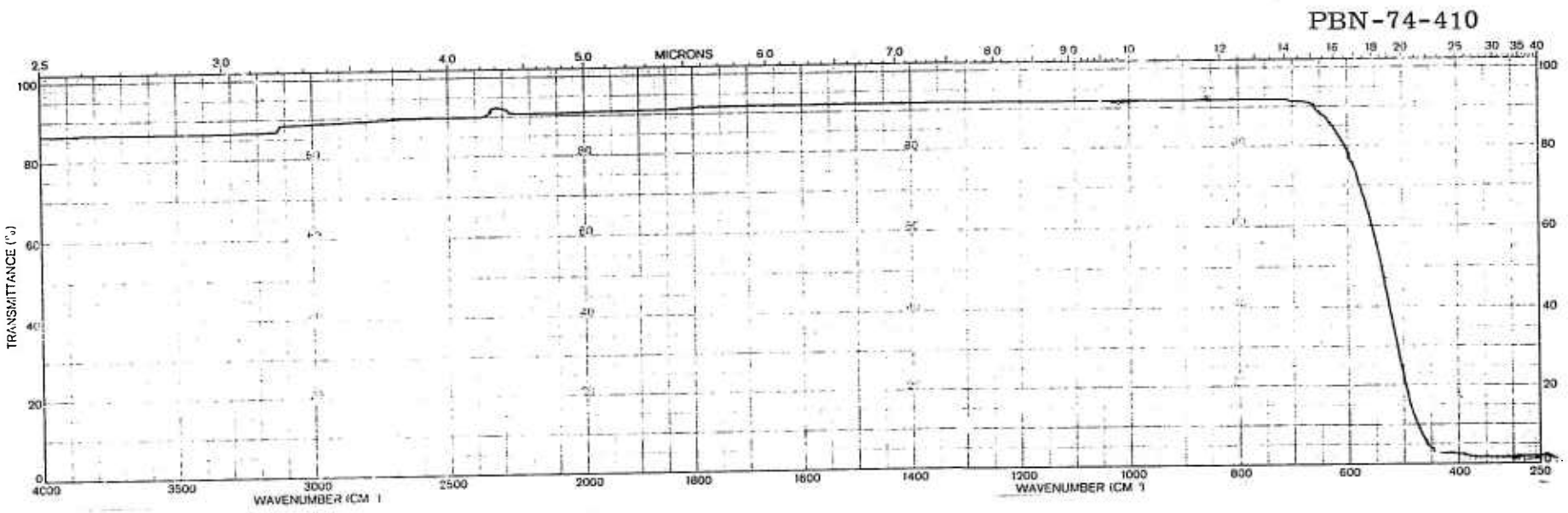

Fig. 6-9 Infrared Spectrum of Sample NPC-40. 200 ppm $SrCl_2$-KCl (Merck). 3.5 cm path length.

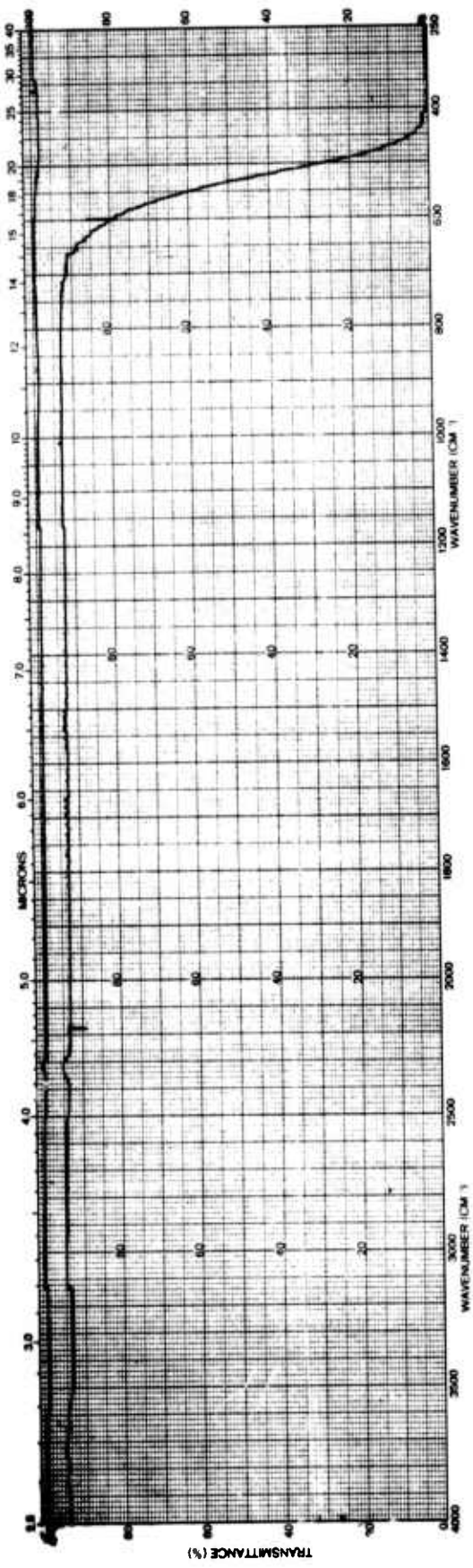

Fig. 6-10 Infrared Spectrum of Sample VHP-213. 200 ppm $SrCl_2$-KCl (Merck). 2.7 cm path length.

TABLE 6-1

ANALYSIS OF KCl CASTINGS AND MERCK "SUPRAPUR" POWDER

Detected Impurities*	Merck Powder	Casting NPC-22	Casting NPC-39	Casting NPC-47
Mg	< 1	1	0.5	1
Al	1-10	1	0.1	5
Si	ND	0.5	0.1	1
K	H	H	H	H
Ca	< 1	2	0.5	0.5
Fe	ND	0.1	ND	0.3
Cu	ND	1	0.5	0.1
Sr	ND	ND	400	300
Mo	ND	5	ND	ND
Pb	ND	.1	ND	0.5
Total Detected Impurities**	3-13	10.7	1.7	8.4

ND ≡ not detected

H ≡ balance

* Results in ppm; 40 additional impurities undetected

** Excluding Sr

and 39 were produced. Casting NPC-22 was undoped while casting NPC-39 was nominally doped at 200 ppm $SrCl_2$. Casting NPC-47 is the RAP-treated one. In general,no impurity pickup was found in the casting process by either analysis (emission spectroscopy performed by Jarrell-Ash, Waltham, Mass.) or by the IR transmission results. And the RAP-treated casting by analysis is as pure as the others.

6.1.4.2 Scattering centers

In order to better understand the apparent 10.6 μm absorption of various castings and single crystals such as casting NPC-40 (Fig. 6-9) which exhibits a high absorption coefficient with no evidence of a band at 10 μm, it was decided to attempt to correlate absorption and optical scatter. Qualitatively it was found that all samples with low 10.6 μm absorption coefficients scattered less in a He-Ne laser beam than did corresponding samples of high absorption coefficients.

As a result, selected samples of doped and undoped KCl (both cast and single crystal) were microscopically examined at 120× with transmitted light. Samples ranged in thickness from 10 to 20 mm and were examined by focusing from one polished surface through the sample to the opposite polished surface. All scattering centers that were microscopically visible were counted. At least four random fields of view for each sample were counted. Comparison between samples could be obtained by defining a scattering number as the total number of counted particles or voids in the total volume examined.

The results are summarized in Table 6-2. It gives the sample, its measured 10.6 μm absorption, β, (from a plot of absorption versus length), and the scattering center density.

The results indicate a semiquantitative correlation between β and scatter. The lower absorption samples have very few microscopically visible inclusions, while the greater the number of inclusions, the higher the absorption coefficient. Of course, the higher absorbing samples may have an impurity band near 10 μm, but not necessarily,as has been seen.

TABLE 6-2

10.6 μm ABSORPTION AND SCATTER

Specimen	$\beta_{10.6\ \mu m}$	Sample Thickness (mm)	Center Density (cc^{-1})
73-85	3.7×10^{-4} cm^{-1}	10	0
73-62	6.1×10^{-4}	15	105
VHP-213	6.3×10^{-4}	27	330
73-50	6.7×10^{-4}	20	0
73-29	7.2×10^{-4}	15	0
NPC-22	7.8×10^{-4}	14	940
73-86	1.5×10^{-3}	6	internal subgrains
72-52	2.4×10^{-3}	16	5300
73-72	3.9×10^{-3}	11	2400
TW4	3.9×10^{-3}	12	> 3900*
NPC-40	4.8×10^{-3}	11	> 3300*
72-61	5.3×10^{-3}	10	5200
TW3	6.3×10^{-3}	10	8800
NPC-31	7.4×10^{-3}	13	> 14,000*
NPC-35	1.3×10^{-2}	11	internal subgrains
NPC-39	1.7×10^{-2}	10	> 14,000*
NPC-36	1.9×10^{-2}	10	> 14,000*

* Very nonuniform from field-to-field.

It is also not yet clear whether the residual absorption (above the intrinsic value for KCl at 10.6 μm) for the best samples is limited by impurity absorption or by scatter. Further work is under way in order to resolve this question.

6.2 Alkaline Earth Fluorides

6.2.1 Cast fluorides

As mentioned before, the main effort during the first quarter of this program was directed toward the fusion casting of the alkaline earth fluorides and primarily of CaF_2. To that end, both of our large furnaces were used, with most of the casting having been done in the vacuum hot press furnace capable of castings up to about 6 inches in diameter. The two-zone furnace was used both as a casting furnace and a vacuum annealing furnace.

Early in the quarter, when the casting of fluorides was first attempted in the two-zone furnace, a major problem developed. At the high temperatures (1400-1500°C) required for the casting of fluorides, alumina reacts in the hot zone with the volatile fluorides. As a consequence, the thermocouples and element supports were rapidly destroyed. The problem appeared to be aggravated by the use of PbF_2 added as a scavenger for the purification of CaF_2. Since the furnace could readily be used at temperature less than 1000°C, strained castings produced in the vacuum hot press were vacuum annealed in the two-zone furnace.

In order to overcome the alumina problem, BeO supports were ordered for delivery during the next quarter. For casting in this interim period, BN parts were fabricated in the laboratory and all thermocouples were sheathed in molybdenum protective tubes. The performance of BN, at the melting temperatures of the fluorides, is presently under evaluation.

In Tables 6-3 and 6-4 are listed the fluoride castings produced in the vacuum hot press (VHP) furnace. The early runs, as noted, were mainly to set conditions for complete unidirectional solidification. To most runs PbF_2 was added (usually 2 percent by weight) for the scavenging of any oxide according to the reaction:

TABLE 6-3

VACUUM HOT PRESS (VHP) CASTINGS
PURE FLUORIDES

VHP No.	Material	Comments
144, 146, 148-151	SrF_2	Each run a remelt of the previous one
145, 147	BaF_2	Castings cracked and full of bubbles
152, 154	CaF_2	Hot forged single crystals at 1000°C
158-162	CaF_2	Large ($5\frac{1}{2}$ in.) castings to set conditions for unidirectional solidification
163-168, 184	CaF_2	Small (3 in.) castings to set conditions
169, 170	CaF_2	Large castings with layer of small bubbles very defined
174, 175	CaF_2	Large castings, experiments with slotted elements
176-178, 180, 189, 192, 194-196, 202, 203	CaF_2	Large castings: excellent castings. 2 percent PbF_2 additions
214, 215	CaF_2	Small castings with 10 percent PbF_2 added. Smaller grain size but cracked
216	CaF_2	Small casting with $7\frac{1}{2}$ percent PbF_2. Cracked

TABLE 6-4

VACUUM HOT PRESS (VHP) CASTINGS

FLUORIDE ALLOYS

VHP No.	Material	Comments
179	CaF_2 + 0.93 percent NaF + 0.26 percent YF_3	Cracked
181	CaF_2 + 0.37 percent NaF + 0.10 percent YF_3	
182	CaF_2 + 0.74 percent NaF + 0.21 percent YF_3	Cracked
183	CaF_2 + 0.19 percent NaF + 0.05 percent YF_3	Cracked
185	CaF_2 + 520 ppm YF_3	Cracked
186	CaF_2 + 930 ppm NaF	
187	CaF_2 + 1860 ppm NaF	
188	CaF_2 + 500 ppm LaF_3	
190	CaF_2 + 1860 ppm NaF	VHP 187 remelted
191	CaF_2 + 200 ppm LaF_3	
193	CaF_2 + 400 ppm LaF_3	

$$PbF_{2(s)} + CaO_{(s)} \rightarrow CaF_{2(s)} + PbO_{(g)}$$

as first used by Stockbarger.[29]

Table 6-3 lists all the pure castings (SrF_2, BaF_2 and CaF_2) produced, while Table 6-4 lists the castings of CaF_2 with various additions of LaF_3, YF_3 and/or NaF. Figure 6-11 shows a polished six-inch window of pure CaF_2 cast in our laboratory illustrating the high optical quality that can be achieved.

The procedure to produce castings in the vacuum hot press furnace is as follows. The charge to be melted (fluoride and scavenger) is loaded in a covered ATJ graphite crucible (either 3 or $5\frac{1}{2}$ in. in diameter) and placed in the furnace. A vacuum is drawn and when it reaches 10^{-4} torr, the furnace is turned on and brought up to temperature in about 2 hours. The charge is held at 1475°C for 1 hour to insure complete melting (temperature is monitored by means of an optical pyrometer). The temperature is then slowly reduced at 5-10°C every 10 minutes to 1365°C, at which time either shutdown or further cooling at faster rates to about 1100-1200°C is initiated. Normally the furnace is shut down at about 1200-1300°C. Cooling to room temperature takes about six hours. Each casting produced by this rapid cooling is highly strained, and care is required in handling to prevent the specimens from cracking. The results with aliovalent doping were universally poor and casting under more carefully controlled cooling conditions will be attempted in the two-zone furnace during the next quarter.

Initially it was decided to use high purity starting material for the castings. Consequently, Optovac single crystal (random cutting) CaF_2 was used, as well as Harshaw single crystal SrF_2 and BaF_2.

Selected samples of these raw materials were analyzed by emission spectroscopy. Table 6-5 gives the results of the analyses on the following samples: Harshaw single crystal SrF_2; a casting of SrF_2 (VHP-144); Harshaw and Optovac single crystal CaF_2; an early casting of CaF_2(HN1-2)

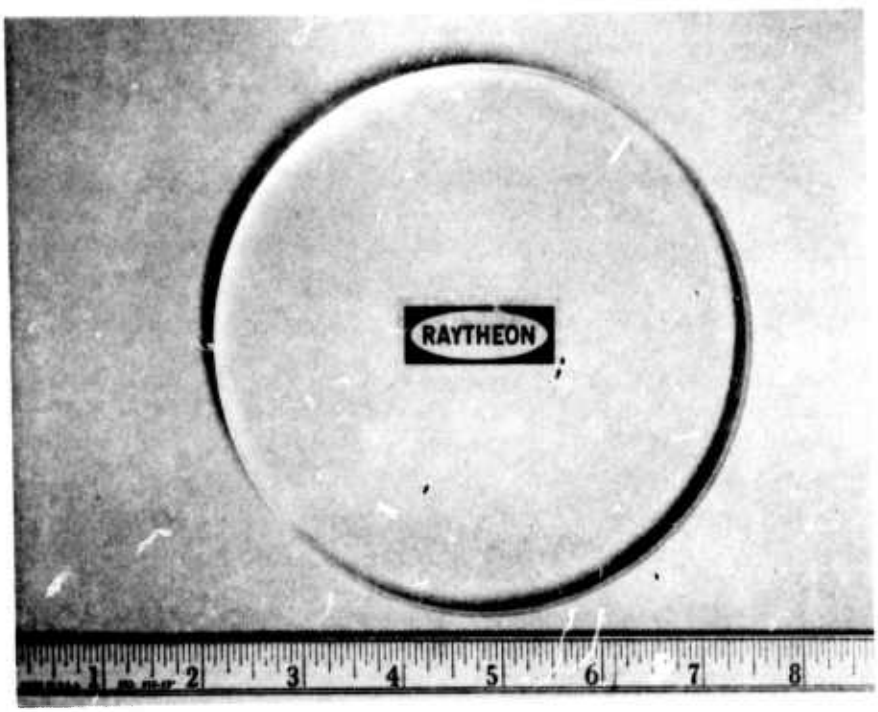

Fig. 6-11 Polished Casting of CaF_2 $5\frac{1}{2}$ in. diameter $\times$ 0.5 in. thick.

TABLE 6-5

ANALYSIS OF PURE SrF_2 AND CaF_2 STARTING CRYSTALS AND CASTINGS

Detected* Impurities	Harshaw SrF_2	Cast SrF_2 (VHP-144)	Harshaw CaF_2	Optovac CaF_2	Casting HN1-2	Casting CF8	Casting CF18
Mg	2	1	10	0.1	0.5	0.5	5
Al	ND	ND	1	0.5	ND	0.1	0.1
Si	0.1	0.1	0.5	0.5	0.1	0.5	0.5
Ca	500	700	H	H	H	H	H
Cr	ND	ND	ND	ND	ND	0.5	ND
Mn	ND	ND	0.1	ND	ND	0.1	ND
Fe	0.05	ND	0.5	0.5	ND	5	0.5
Ni	ND	ND	ND	ND	ND	5	1
Cu	0.01	0.05	0.1	0.1	0.5	50	1
Sr	H	H	ND	ND	ND	ND	ND
Ag	0.05	0.05	ND	ND	ND	ND	ND
Ba	1	ND	ND	ND	ND	ND	ND
Pb	ND	ND	ND	ND	ND	0.5	ND
Total Impurities Delected**	3.2	1.2	12.2	1.7	1.1	62.2	8.1

ND ≡ not detected

H ≡ balance

* 37 additional elements undetected, results in ppm

** Excluding Ca in the SrF_2 samples

in the vacuum hot press furnace; and two castings of CaF_2 (CF8 and CF18) produced in the two-zone furnace at the time the alumina reaction problems were discovered in that furnace. From the analyses, it is clear that casting in the vacuum hot press furnace does not degrade the purity of the starting material. However, in the two-zone furnace, an increase in impurities did occur.

6.2.2 Hot forging

During the first quarter only two hot forgings of single crystal CaF_2 were attempted as listed in Table 6-3. Both were quite successful. Figure 6-12 shows VHP-154, a hot forging done at 1000°C in the vacuum hot press. A 1 in.-diameter Optovac single crystal was hot forged to 79 percent reduction in thickness. Resultant grain size, however, is large, as seen in Fig. 6-13, due to the high forging temperature.

6.2.3 Strain annealing

The major problems with the casting of the fluorides during the first quarter were the high residual strains due to rapid cooling in the vacuum hot press furnace, and the resulting susceptibility to cracking. Early in the quarter, a strain anneal procedure was developed. Figure 6-14 shows qualitatively the results of strain reduction (as viewed through crossed polarizers) by vacuum annealing one CaF_2 casting in the two-zone furnace. Figure 6-14a shows the as-cast sample (from which pieces have been cut). Figure 6-14b shows some strain reduction by a vacuum anneal at 500°C for 10 hours, followed by cooling to room temperature at 25°C/hour. Figure 6-14c shows the sample reannealed at 1000°C for 10 hours, followed by cooling at 25°C/hour. In this case, the sample is quite free of residual strain. Figures 6-15a and 6-15b show another casting of CaF_2 both as-cast and annealed at 1000°C for 7 hours and cooled at 25°C/hour.

As a result of the success of these early strain anneals, several large castings were similarly annealed to give strain-free samples for polishing (Fig. 6-11) and testing.

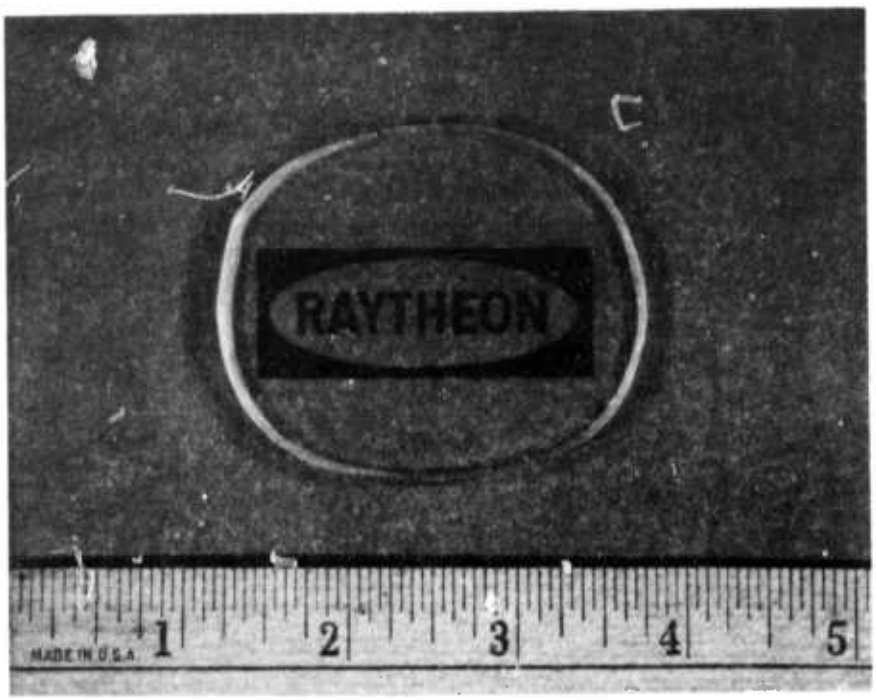

Fig. 6-12 CaF_2 Single Crystal Hot Forging. Sample VHP-154. Forged at 1000°C to 79 percent reduction.

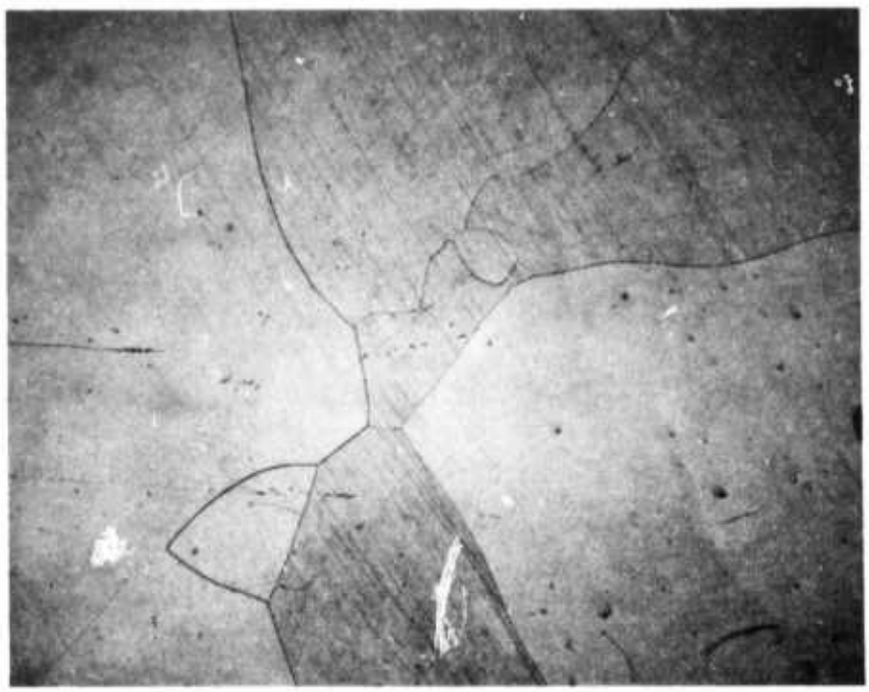

Fig. 6-13 Photomicrograph of VHP-154. Hot Forged CaF_2 at 1000°C 79 percent reduction in thickness. 25X

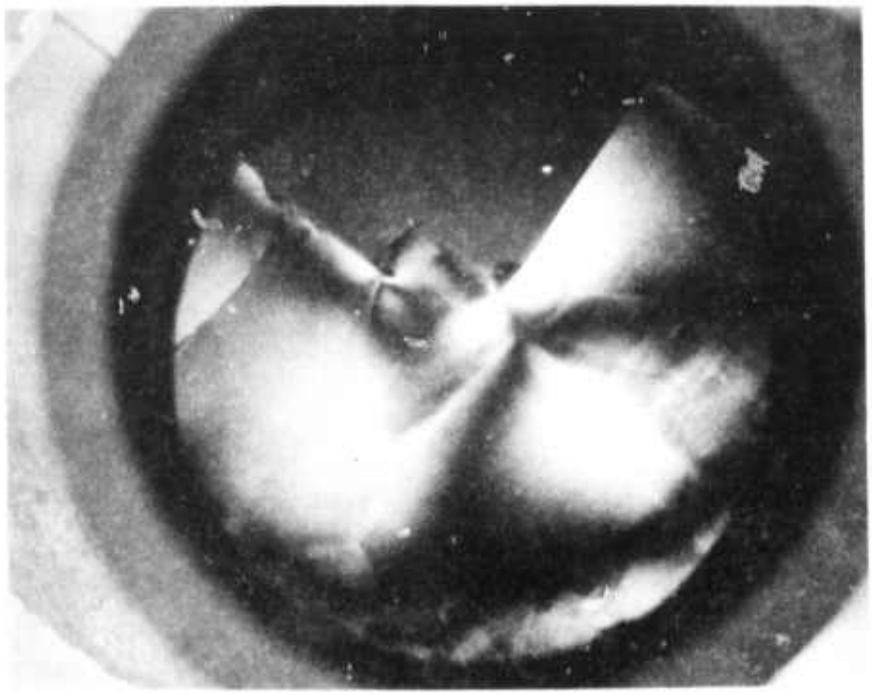

Fig. 6-14a CaF_2 As Cast. Viewed through crossed polarizers.

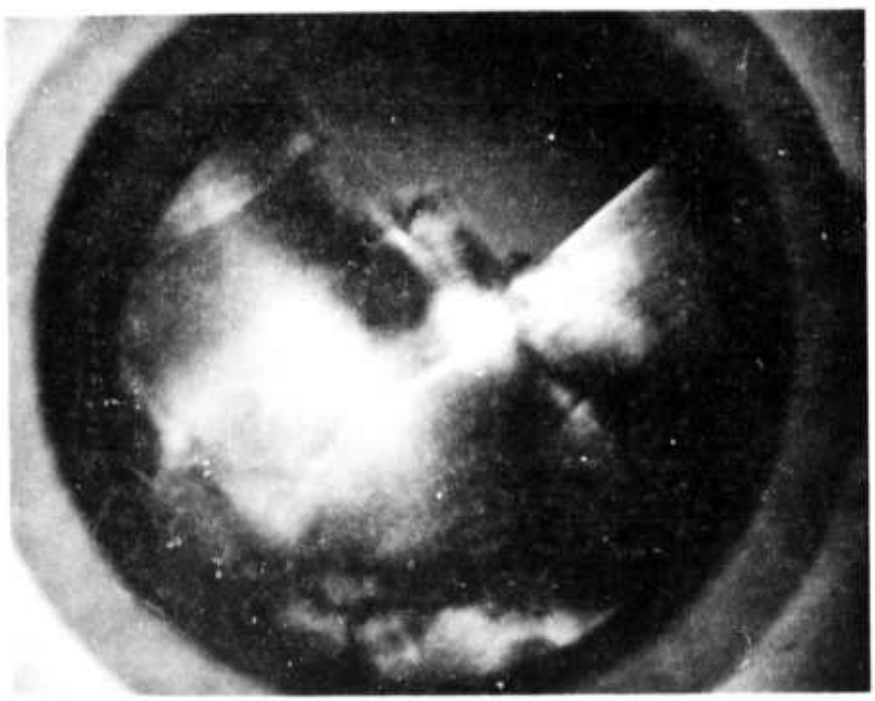

Fig. 6-14b Same. 500°C anneal for 10 hrs. and cooled at 25°C/hr.

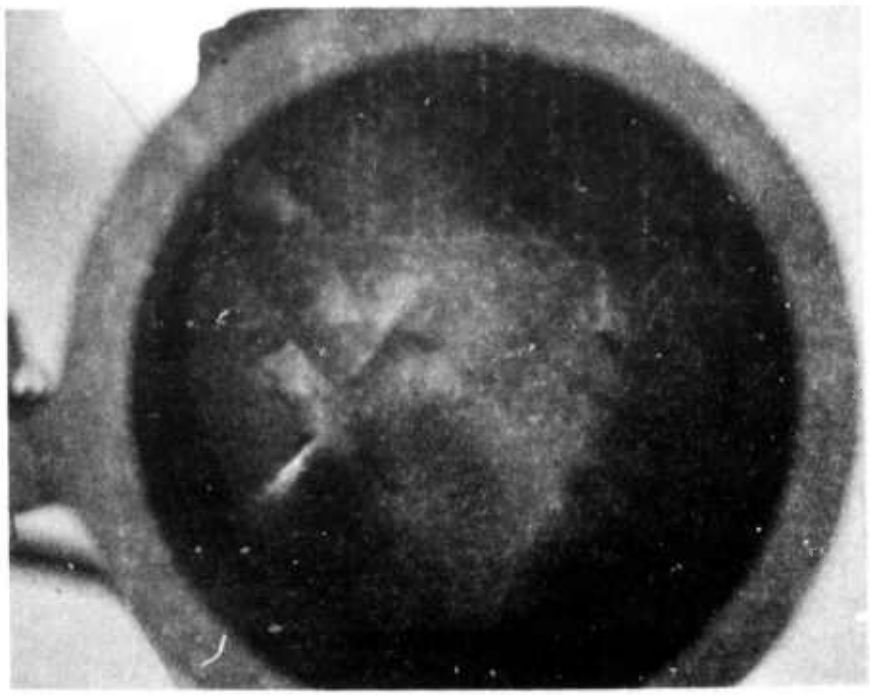

Fig. 6-14c Same. 1000°C anneal for 10 hrs. and cooled at 25°C/hr.

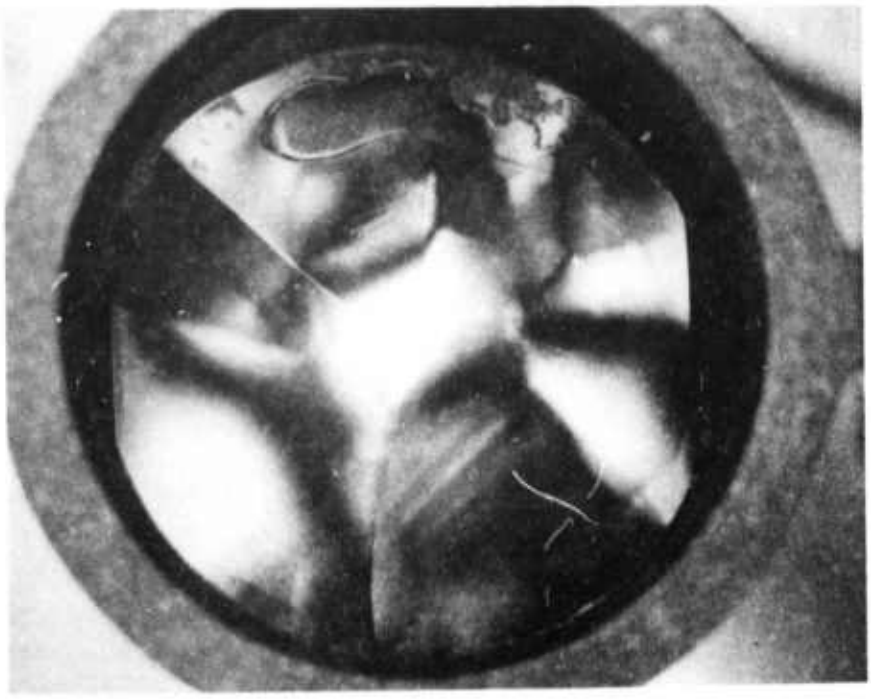

Fig. 6-15a Cast CaF_2 (VHP-167), As Cast. Viewed through crossed polarizers.

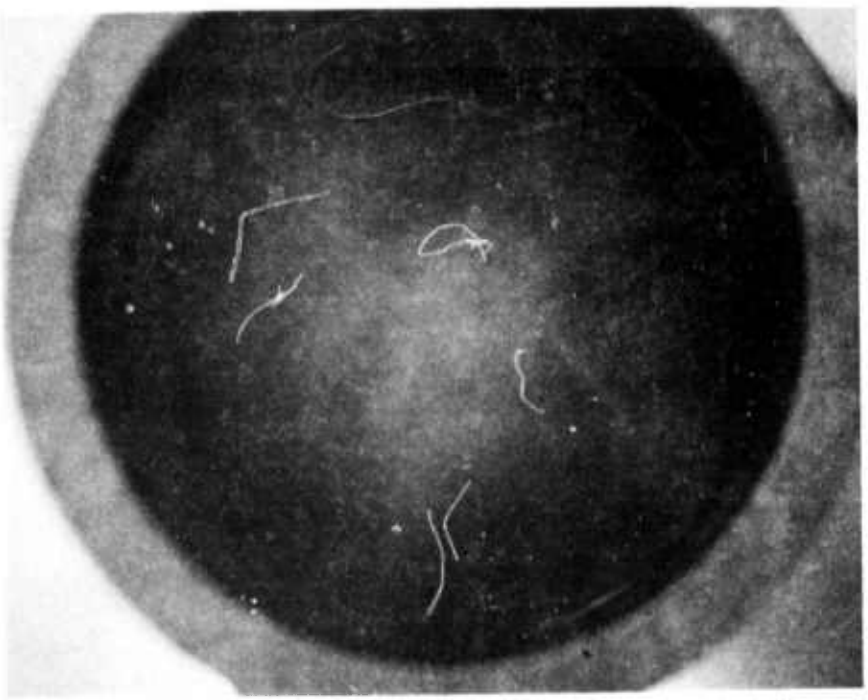

Fig. 6-15b Same After 1000°C Anneal for 10 hrs. and Cooled at 25°C/hr.

Only late in the quarter, as will be discussed below, was it discovered that the annealing procedure degraded the optical properties (i.e., 5.25 μm absorption) by a precipitation and scatter problem. During the next quarter, the inter-relation between strain relief annealing and the development of scattering centers will be investigated more fully.

6.2.4 Optical properties and scattering

The feasibility of casting high purity CaF_2 has been demonstrated this first quarter by using high purity starting material. Figures 6-16 and 6-17 show respectively the IR transmission spectra for an Optovac single crystal of CaF_2 used as starting material and a CaF_2 casting (VHP-167), with no detectable differences in the two. No impurity bands are detectable in either spectrum. The 5.25 μm absorption coefficients for these two samples are 4.9×10^{-4} cm^{-1} and 4.8×10^{-4} cm^{-1}, respectively. These absorption coefficients at 5.25 μm were measured using a CO laser calorimeter, and no surface loss corrections have been made (no absorption vs length measurements have been made). Clearly, the results show that the fusion casting process does not degrade the optical properties of the starting materials.

Figure 6-18 shows the IR transmission curves for samples of Harshaw single crystal SrF_2 and a casting (VHP-151) of SrF_2. Again no detectable differences can be noted nor are any impurity bands present in either sample. However, the laser-measured 5.25 μm absorption coefficient for the Harshaw single crystal material is 5.3×10^{-4} cm^{-1}, at least 5 times the intrinsic value. Absorption coefficient measurements on cast SrF_2 are in progress.

Early in the casting of CaF_2, it was noticed that in random castings a bubble layer (or region) occurred about half way into the casting in a plane perpendicular to the freezing direction. It was even observed in several samples that some preferred orientation of these tiny bubbles occurred. In most cases, the bubble layer of these castings could be cut away leaving very good material in the bottom section. The reasons for the tiny bubbles is unclear and will be investigated further.

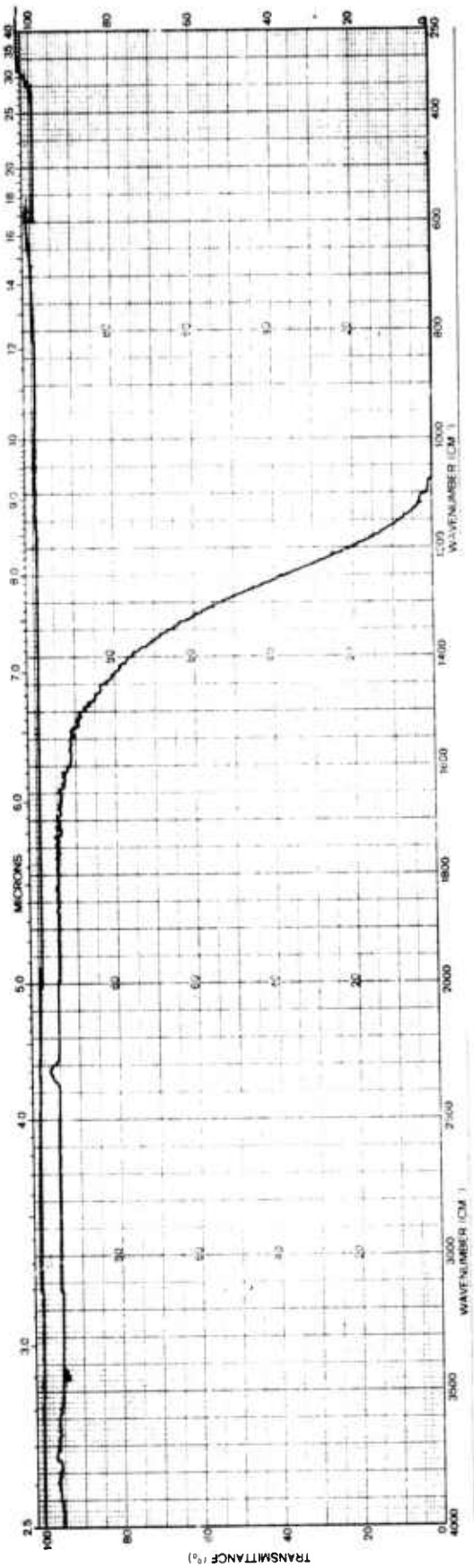

Fig. 6-16 Infrared Spectrum of Sample Optovac CaF_2 Single Crystal. 5.8 cm path length.

PBN-74-409

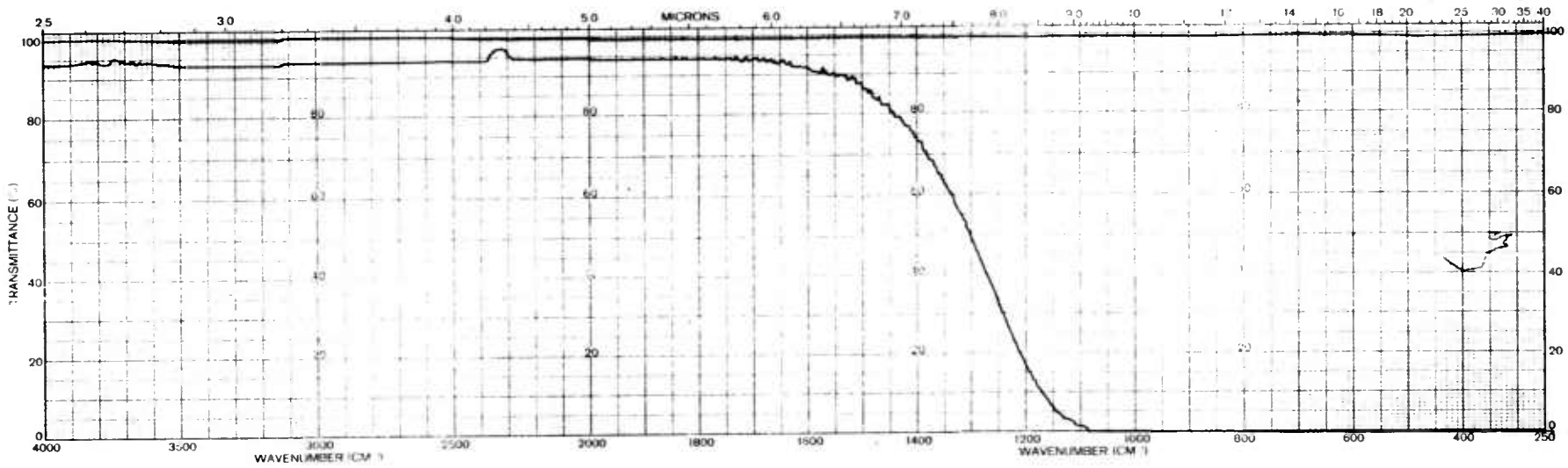

Fig. 6-17 Infrared Spectrum of Sample VHP 167, Cast CaF_2. 6.5 cm path length.

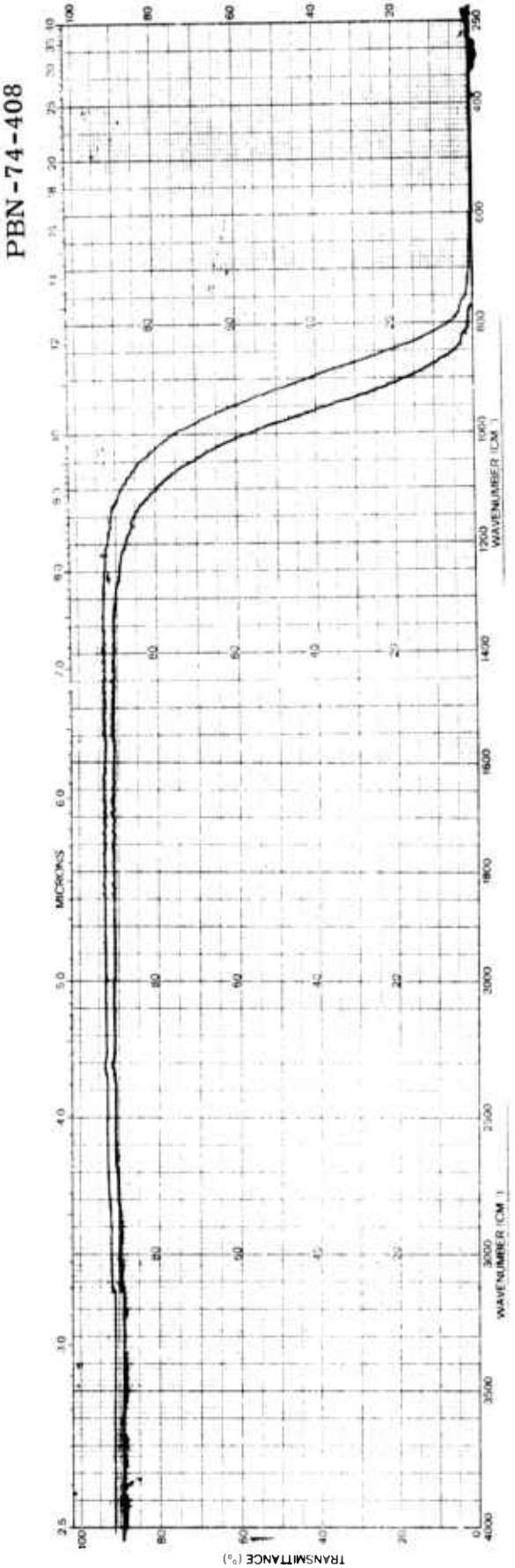

Fig. 6-18 Infrared Spectra of Sample VHP-151 (top), SrF_2 Casting: 7 mm path length and Harshaw (bottom), Single crystal SrF_2: 12 mm path length.

The effect of these tiny bubbles on the optical properties of the castings are shown in Table 6-6. These results indicate qualitatively the effect of scatter centers on 5.25 μm absorption. Three measurements were made on a casting in which there was a region of bubbles. In the region with no bubbles and least scatter, a good 5.25 μm absorption coefficient of 5.7×10^{-4} cm^{-1} was measured. Nearer the bubbly region, a slightly higher absorption occurred, while directly through the bubbly region (high scatter), a high apparent absorption coefficient of 2.3×10^{-3} cm^{-1} was measured.

The scatter results can also be graphically seen in Fig. 6-19. This figure shows two CaF_2 castings, one with (VHP-194) and one without (VHP-167) scattering as viewed with a He-Ne laser beam. The specimen with scattering has a measured 5.25 μm absorption coefficient of 2.0×10^{-3} cm^{-1} (average of 3 samples from one large casting), while the scatter free sample has the above mentioned β of 4.8×10^{-4} cm^{-1}.

Scattering is clearly a serious problem and its development during strain annealing requires further investigation. The effect of annealing is shown in Fig. 6-20. This figure shows the formerly scatter-free casting (Fig. 6-19) after the typical anneal at 1000°C for 7 hours followed by cooling at 25°C/hour. Again a He-Ne laser beam is directed through the interior of the sample. Figure 6-20a shows the high degree of scatter now in the sample produced during the anneal. The two figures together show the nature of preferred orientation of the scattering centers. Figure 6-20b shows the same sample but with the specimen rotated by about 20°. Much less scatter is apparent.

The scatter also degraded the optical properties of the annealed castings. For this sample (VHP-167), as annealed and with scatter, the 5.25 μm absorption coefficient is 8.0×10^{-4} cm^{-1}, an increase of about 70 percent over its scatter-free (and unannealed) absorption. Similarly, another sample (HN1 of Table 6-6) was annealed and the resultant absorption degradation noted, an increase of about 90 percent to 1.1×10^{-3} cm^{-1} from 5.7×10^{-4} cm^{-1}.

TABLE 6-6

APPARENT ABSORPTION COEFFICIENTS AND SCATTERING

CaF_2 CASTING HN1

5.25 μm Absorption Coefficient	Location in Sample
5.7×10^{-4} cm^{-1}	through clear area
6.6×10^{-4} cm^{-1}	near bubbles
2.3×10^{-3} cm^{-1}	through bubbles

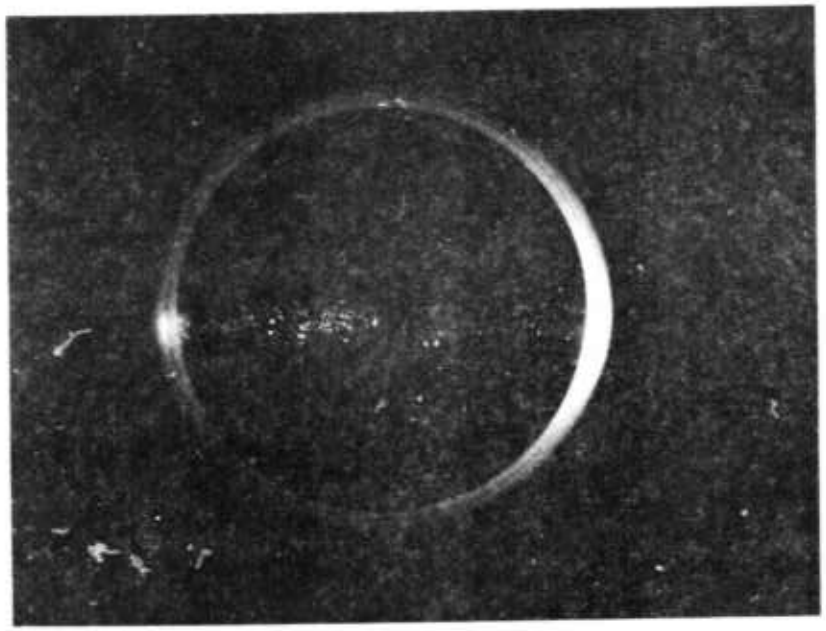

CaF_2 Casting with Scattering

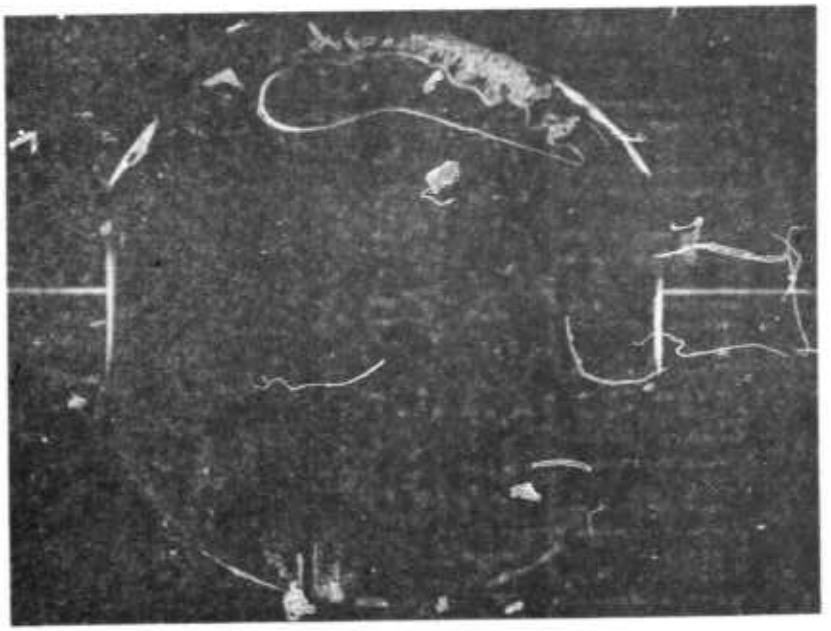

CaF_2 Casting without Scattering

Fig. 6-19 Left. Sample of cast CaF_2 (VHP-194) showing scatter.
Right. Sample of cast CaF_2 (VHP-167) showing no scatter.

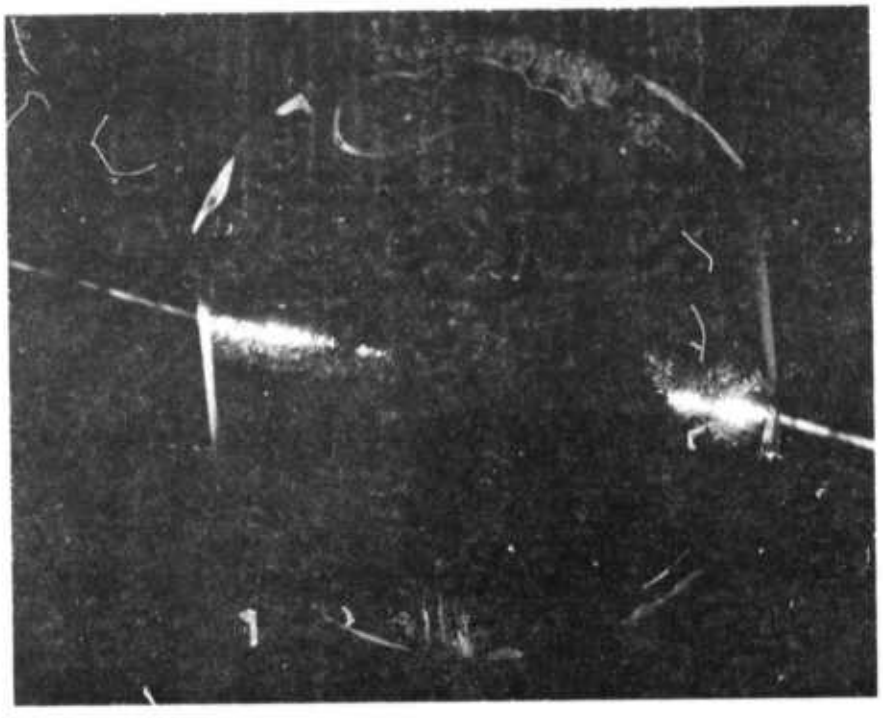

Fig. 6-20a Scattering in Cast CaF_2 (VHP-167) After Annealing.

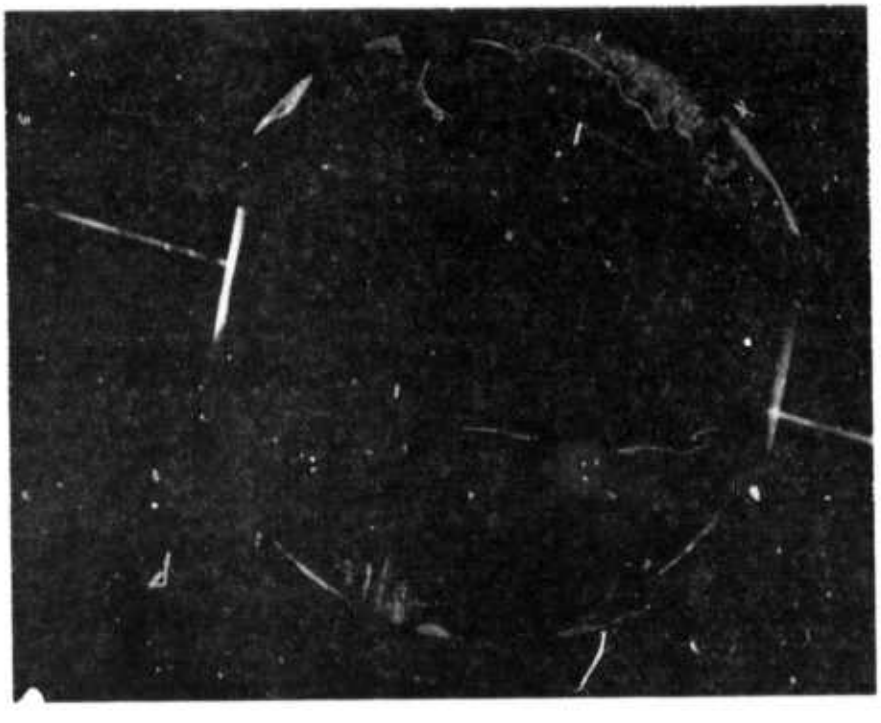

Fig. 6-20b Same Only Rotated About 20°.

Figure 6-21 shows graphically some of scattering centers in VHP-167 after annealing. The micrograph was taken in transmitted light and focussed in the interior of the sample; it shows the preferred orientation of these scattering centers which are about 100 μm long. It has not yet been established what the scattering centers are, but there is some evidence that they are platelets (viewed on edge in Fig. 6-21). Figure 6-22 shows types of scattering centers present in another annealed sample (VHP-194). These were found in a more random nature, and show an elongated bubble as well as faceted inclusions. Figure 6-23 clearly shows two of these faceted inclusions just beneath a {111} cleavage plane of CaF_2. The three-fold symmetry strongly suggests that these may be "negative" crystals or bubbles. These are presently being analyzed to detect their chemical composition.

To date, no single crystal starting material has been annealed. It is therefore unclear whether the scattering centers are a problem of impurity pickup (undetectable by analysis) in the casting process, during the annealing procedure, whether it is caused by a residual impurity precipitation process, or precipitation of excess vacancies produced during annealing. Experiments are underway to resolve the question.

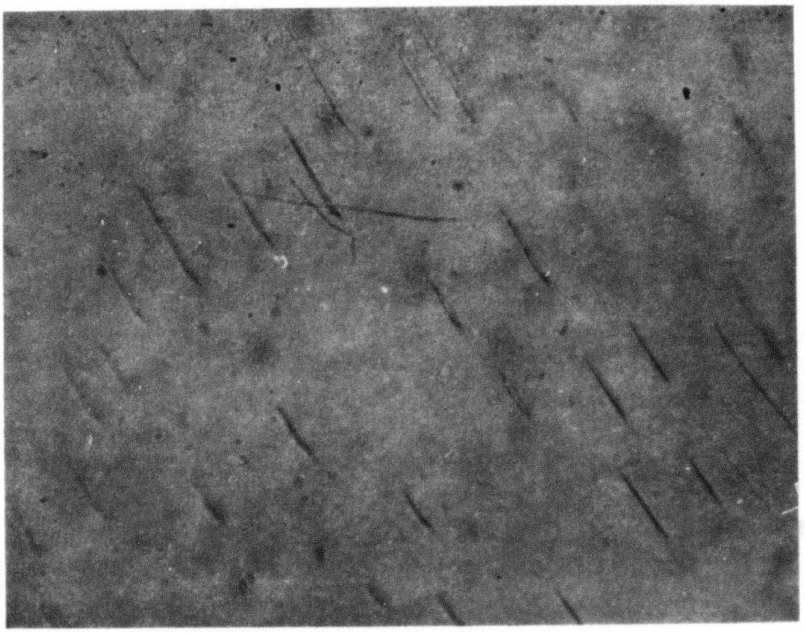

Fig. 6-21 Scattering Centers in Cast CaF_2 (VHP-167) After Annealing. Transmitted light. 100×

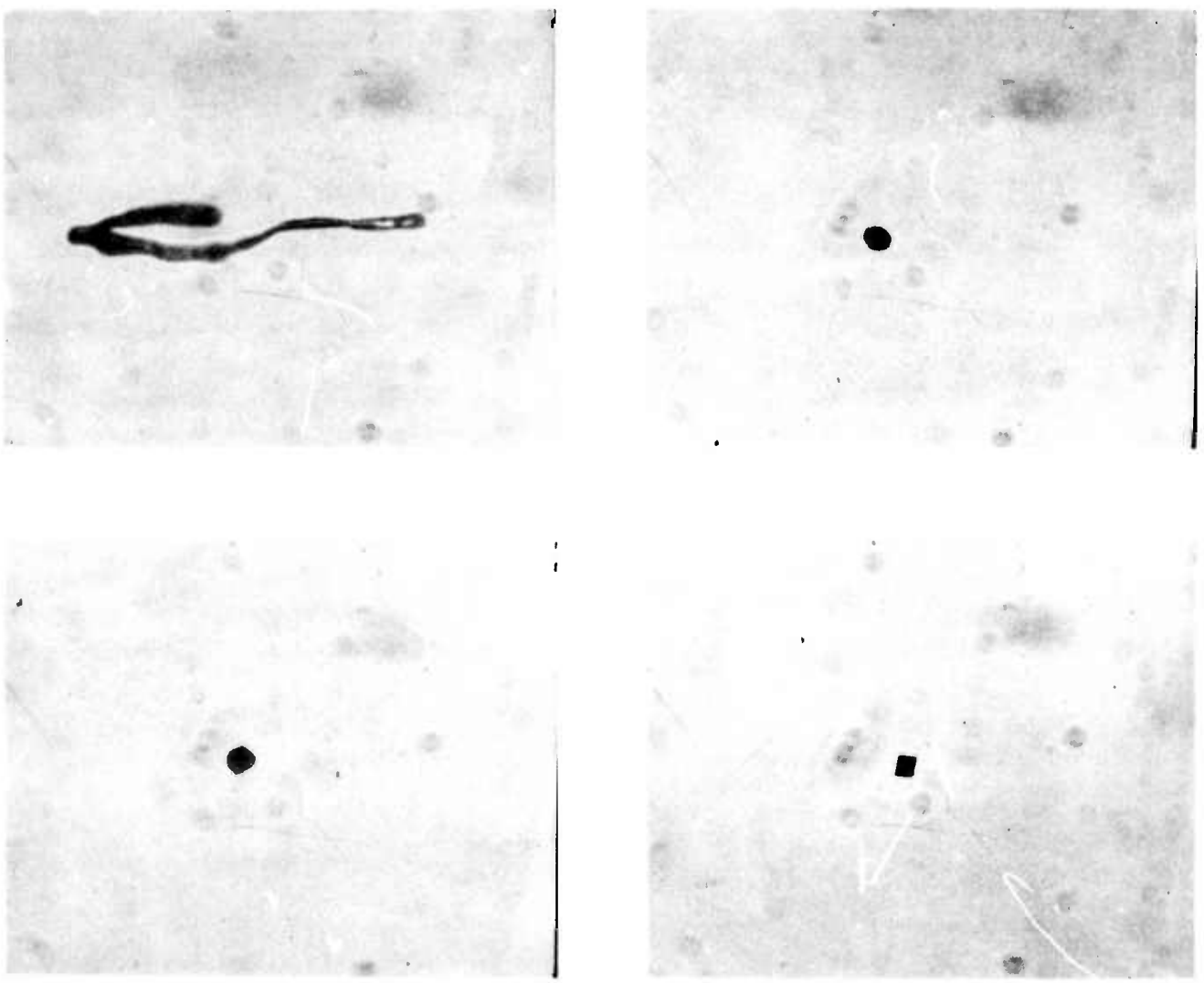

Fig. 6-22 Scattering Centers in Cast CaF_2.

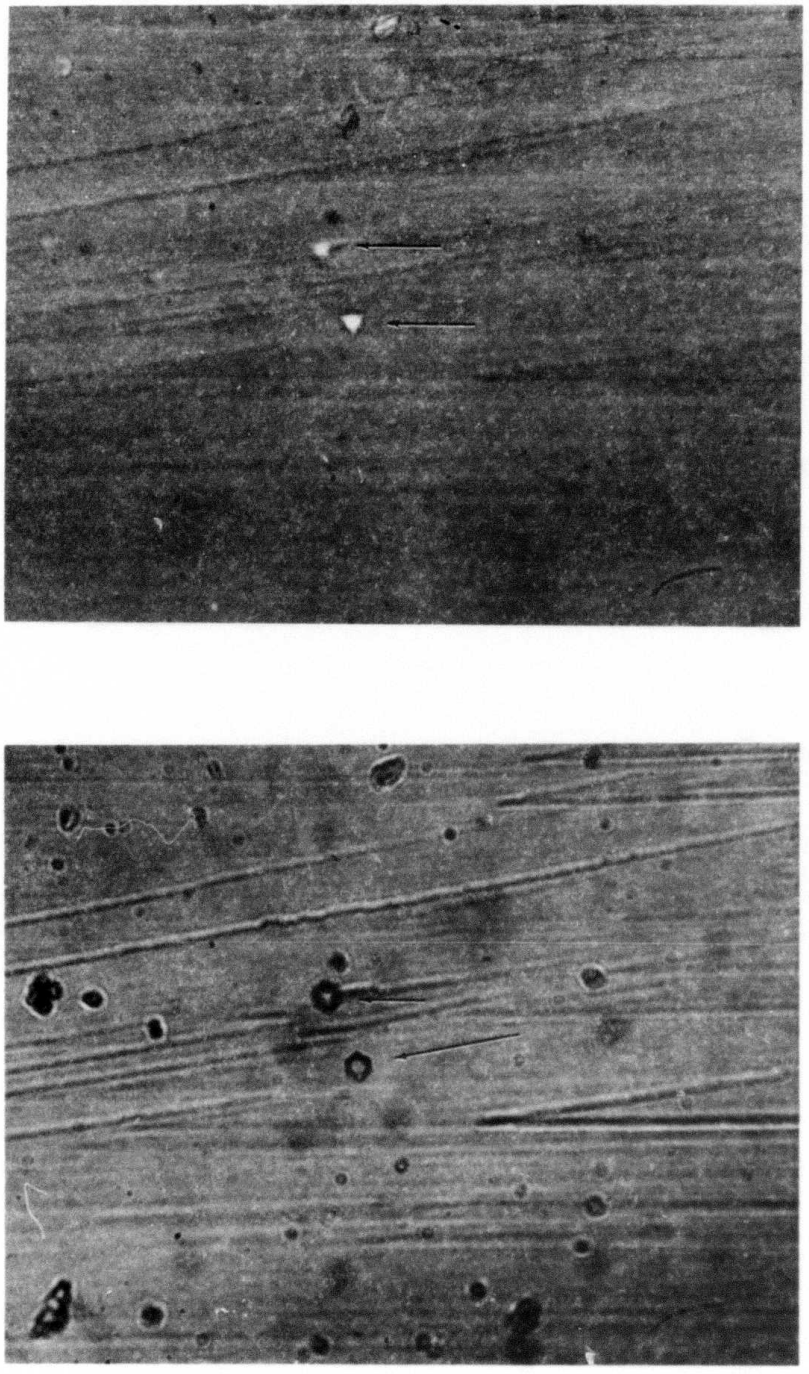

Fig. 6-23 Scattering Centers (arrows) Just Below Cleavage Surface in Cast CaF_2. Top: incident illumination. Bottom: transmitted illumination.

7.0 SUMMARY AND CONCLUSIONS

7.1 Alkali Halides

7.1.1 TTT data

Time-temperature-transformation curves for precipitation and attendant hardness reduction in KCl-$SrCl_2$ alloys have been completed. The results indicate that for less than about 800 ppm $SrCl_2$ in solid solution, it should be possible to cool alloys to room temperature without precipitation.

7.1.2 Thermal conductivity

Thermal conductivity data obtained on KCl-$SrCl_2$ alloys were not sufficiently precise to determine the effect of $SrCl_2$ doping on conductivity. These experiments are being repeated.

7.1.3 Strain removal

Residual strain in KCl castings has been successfully removed by an appropriate annealing and cooling cycle.

7.1.4 Optical properties

7.1.4.1 RAP processing

Reactive atmosphere processing (RAP) of "reagent" grade starting material was successful in removing impurity bands in the infrared. However, the broad absorption band centered near 10 μm was not completely removed. Further work on RAP processing will be carried out.

7.1.4.2 10.6 μm absorption and scattering

Many samples which do not exhibit the broad 10 μm absorption band still can have a high 10.6 μm absorption coefficient. Preliminary data indicated that this high apparent absorption coefficient can be correlated with scattering centers in the bulk.

7.2 Alkaline Earth Fluorides

7.2.1 Casting

As expected, the fluorides are easier to cast than the halides. Castings up to six inches in diameter have been successfully fabricated. Chemical analysis indicates that the purity of the castings is equivalent to that of the starting materials.

7.2.2 Hot forging

Preliminary hot forgings of single crystal CaF_2 have been made at 1000°C. At this temperature a very large grain size results.

7.2.3 Optical properties

5.3 μm calorimetric absorption coefficients of cast CaF_2 have been obtained in the mid 10^{-4} cm^{-1} range. Qualitative correlation between scattering center density and apparent absorption coefficient have been obtained in the fluorides similar to the results with the halides.

7.2.4 Stress relief

Annealing at 1000°C and slow cooling successfully removes residual stress in cast CaF_2 ingots. However, the annealing is accompanied by a large increase in the apparent 5.3 μm absorption coefficient and a significant increase in scatter center density.

8.0 PLANS FOR NEXT QUARTER

During the second quarter the areas of major effort will be the following:

1. Resolve the problem of cracking of castings of annealed $SrCl_2$-KCl during grinding and polishing.

2. Continue to evaluate scatter in both the halide and fluoride castings.

3. Continue efforts in the purification of both KCl and CaF_2 so that high purity starting materials are not required.

4. Determine the optimum annealing procedure for the CaF_2 castings without any degradation of optical properties.

5. Evaluate the mechanical properties of the fluoride castings.

6. Continue to cast high purity halides and fluorides.

9.0 REFERENCES

1. P.A. Miles, D.W. Readey and R. T. Newberg, "Research on Halide Superalloy Windows," Rept. No. AFCRL-TR-73-0758 (October 1973).

2. D.W. Readey and P.A. Miles, "Polycrystalline Halides as Optical Materials," Proc. Conf. on High Power Laser Window Materials, (October 30 - November 1, 1972) p. 507, Report No. AFCRL-TR-73-0372 (19 June 1973).

3. D.W. Readey, R.T. Newberg and P.A. Miles, "The Properties of KCl-$SrCl_2$ Alloys and Their Fabrication by Casting," Proc. Third Conf. on High Power Laser Window Materials, (November 12 - 13, 1973), p. 555, Report No. AFCRL-TR-74-0085 (14 February 1974).

4. F.A. Horrigan, R.I. Rudko, Final Report, "Materials for High-Power CO_2 Lasers," Contract No. DAAH01-69-C-0038 (September 1969), AD693311.

5. F.A. Horrigan, T. Deutsch, Final Report, "Research in Optical Materials and Structures for High-Power Lasers," Contract No. DAAH01-70-C-1251 (September 1971) AD 888788L.

6. F.A. Horrigan and T.F. Deutsch, Prof. Conf. on High Power IR Laser Window Materials, AFCRL Special Report No. 127 (1972).

7. M. Sparks, The Rand Corporation, WN-7243-PR (April 1971).

8. M. Sparks, The Rand Corporation, WN-7296-PR, (April 1971).

9. C.C. Klick, "High Energy Laser Windows," ARPA Order No. 2031, Qtrly. Report No. 1 (NRL, Washington, D.C.) (April 1972).

10. W.L. Phillips, Jr., "Deformation and Fracture Processes in Calcium Fluoride Single Crystals," J. Am. Ceram. Soc. 44 (10) 499 (1961).

11. R.N. Katz and R.L. Coble, "Dislocation Etch Pits and Evidence of Room Temperature Microplasticity in SrF_2 Single Crystals," J. Appl. Phys. 41 (4) 1871 (1970).

12. T.S. Liu and C.H. Li, "Plasticity of Barium Fluoride Single Crystals," J. Appl. Phys. 35 (11) 3325 (1964).

13. G.W. Groves and A. Kelly, "Independent Slip Systems in Crystals," Phil. Mag. 8, 877 (1963).

14. A.G. Evans, C. Roy and P.L. Pratt, "The Rule of Grain Boundaries in the Plastic Deformation of Calcium Fluoride," Proc. Brit. Ceram. Soc. 6, 173 (1966).

15. J. Weertman and J.R. Weertman, "Mechanical Properties, Mildly Temperature-Dependent," Chap. 15 in Physical Metallury, (R.W. Cahn, ed., North Holland Publ. Co., Amsterdam), (1965).

16. J.R. Low, Jr., "The Fracture of Metals," Progress in Materials Science, 12, No. 1 (1963).

17. R.W. Rice, "Analysis of Tensile Strength-Grain Size Effects in Ceramics," Am. Ceram. Soc. Bull. 50, 374 (1971). (Abstract of paper presented at the 73rd Annual Meeting of the American Ceramic Society, April 24-29, 1971).

18. A.G. Evans, "Dislocation Interactions in Ceramic Materials," Proc. Brit. Ceram. Soc. 15, 113 (1970).

19. J.J. Gilman, "Mechanical Behavior of Ionic Crystals," Chap. 4 in Progress in Ceramic Science, 1, 146 (J.E. Burke, ed., Pergamon Press, N.Y.) (1961).

20. G.A. Keig and R.L. Coble, "Mobility of Edge Dislocation in Single-Crystal Calcium Fluoride," J. Appl. Phys. 39, 6090 (1968).

21. R.N. Katz and R.L. Coble, "Effect of Neodymium on Dislocation Velocity in CaF_2," J. Appl. Phys. 45, 2382 (1974).

22. R.L. Fleischer, "Solution Hardening by Tetragonal Distortions: Application to Irradiation Hardening in F.C.C. Crystals," Acta. Met. 10, 835 (1962).

23. J. Short and R. Roy, "Confirmation of Defect Character in Calcium Fluoride-Yttrium Fluoride Crystalline Solutions," J. Phys. Chem. 67 (9) 1861 (1963).

24. A.K. Cheetham, et al., "Defect Structure of Fluorite Compounds Containing Excess Anions," Solid State Comm. 8, 171 (1970).

25. E.M. Levin, C.R. Robbins and H.F. McMurdie, Phase Diagrams for Ceramists, (The Am. Cer. Soc., Columbus) (1964).

26. Hj. Matzke, "Fluorine Self Diffusion in CaF_2 and BaF_2," J. Of Materials Sci. 5, 831 (1970).

27. K. Muto and K. Awazu, "Oxygen Penetration into CaF_2:Sm^{2+} Crystals," J. Phys. Chem. Solids 29, 1269 (1968).

28. E.G. Chernevskaya and Z.N. Korneva, "The Production of Fluorite Crystals in an Atmosphere Containing Fluorine," Sov. J. of Optical Tech. 39, 213 (1972).

29. D.C. Stockbarger, "Artificial Fluorite," J. Opt. Soc. Am. 39, 731 (1949).